

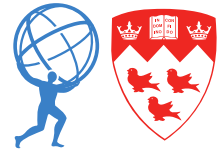
Highlights from the ATLAS experiment

Heather Russell, McGill University

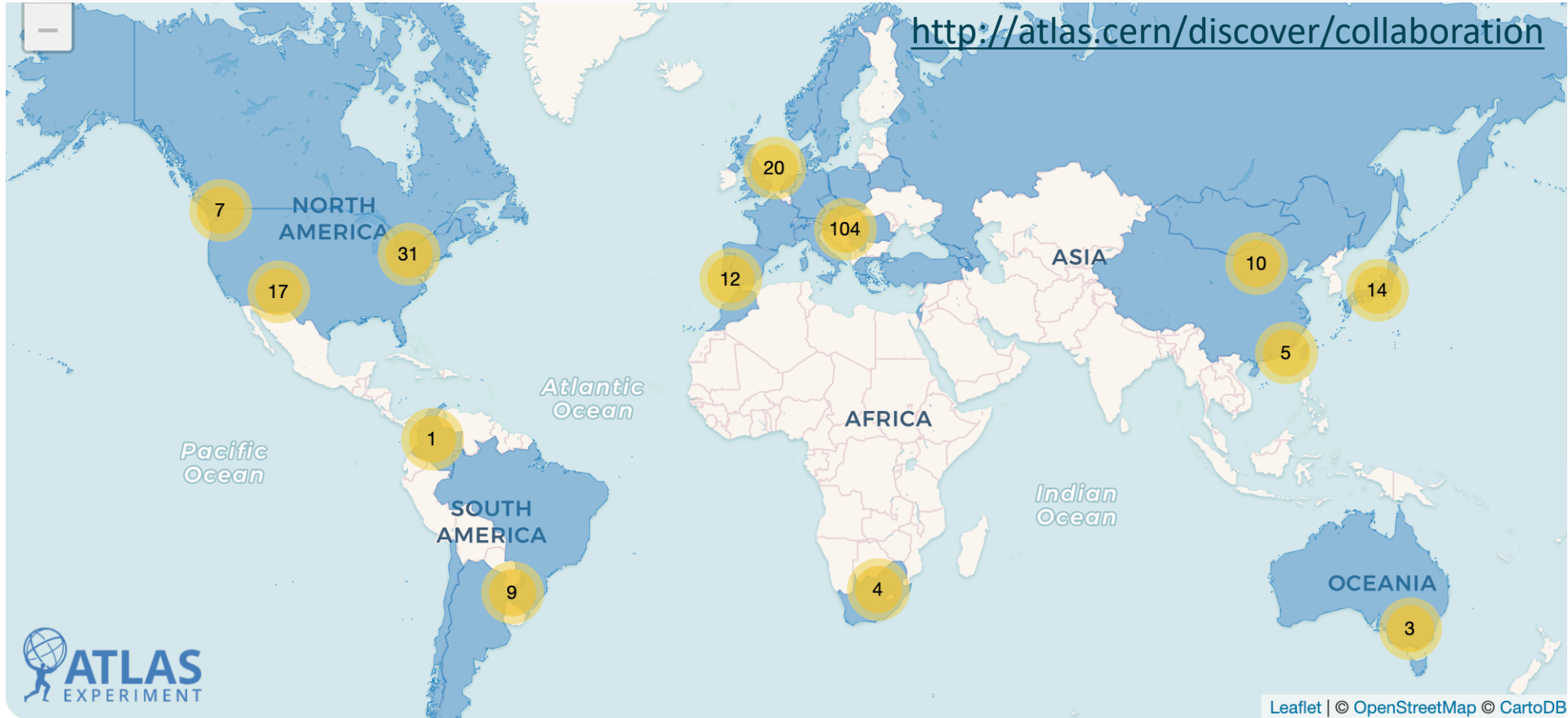
CAP-PPD 2020 – 8 – 9 June 2020



The ATLAS collaboration



<http://atlas.cern/discover/collaboration>



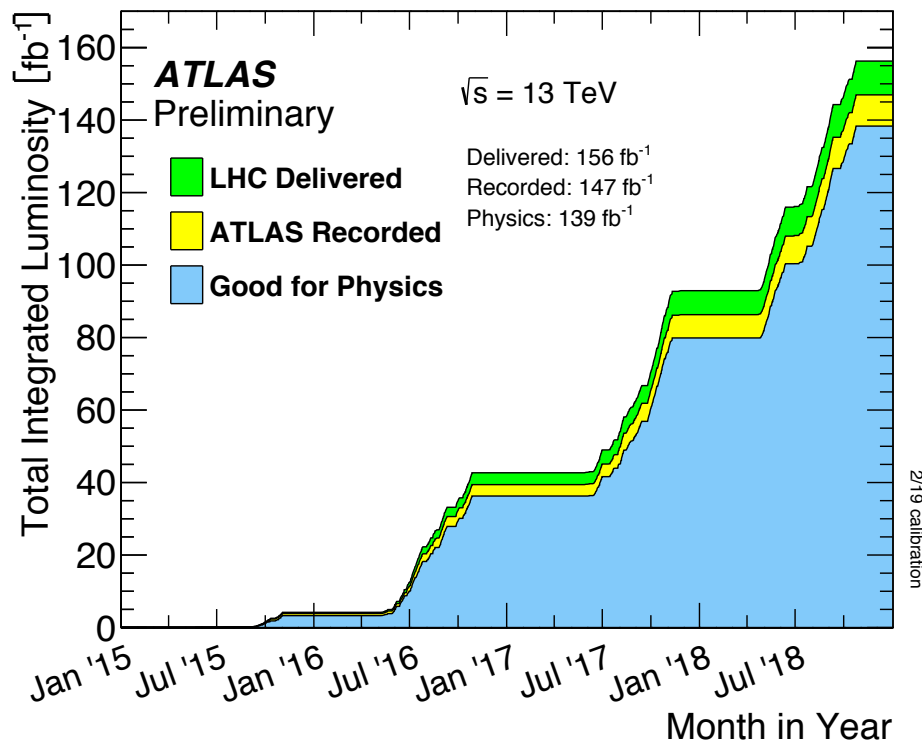
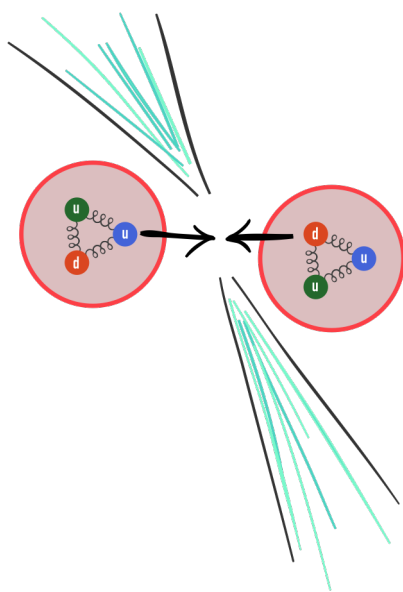
Leaflet | © OpenStreetMap © CartoDB



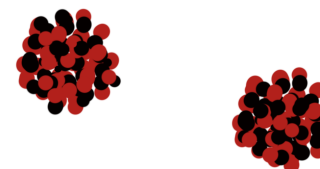
Overview of datasets



139 fb⁻¹ of 13 TeV proton-proton collision data collected from 2015-2018

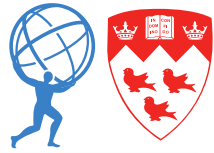


But also special low-pileup data, 5 TeV proton-proton collision data, proton-lead, lead-lead collisions, and xenon-xenon collisions, and more!



<https://twiki.cern.ch/twiki/bin/view/AtlasPublic/LuminosityPublicResultsRun2>

A tour of ATLAS physics*



*with proton-proton collisions

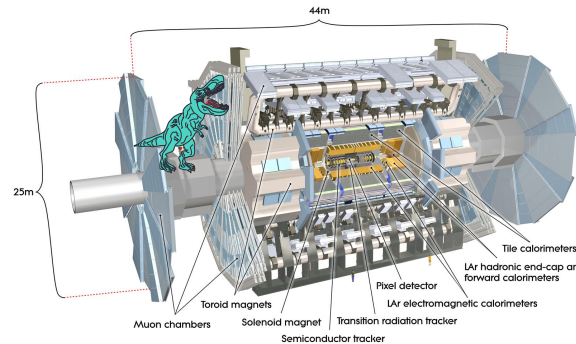
Precision measurements of the Standard Model

Studies of top quark properties

Searches for rare standard model processes

Studies of beauty and charm physics

Studies of Higgs boson properties



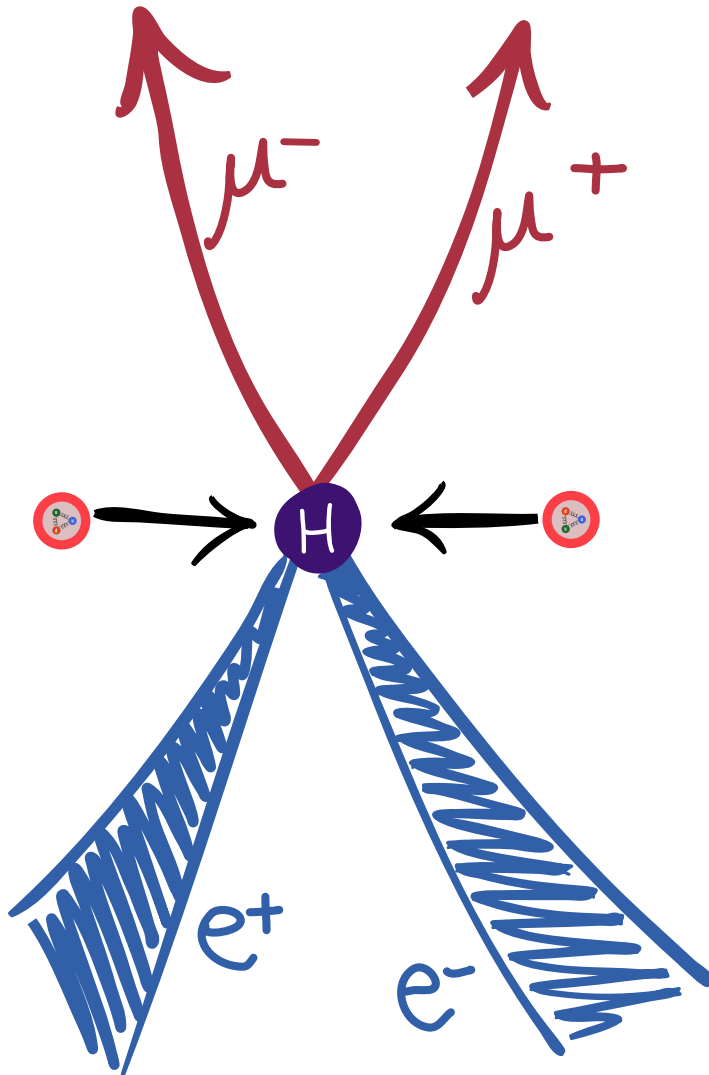
Searches for new physics

Searches for supersymmetry

Searches for exotic Higgs boson decays

Searches for dark matter

Searches for unconventional signatures



Higgs $\rightarrow ZZ^*$ measurements

•————•

Two same-flavour,
opposite-charge lepton
pairs:

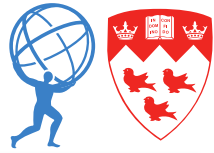
$$2e2\mu, 2e2e, 2\mu2\mu$$

One SFOC pair close to
the Z-boson mass

Four-lepton mass close to
the Higgs boson mass

Overview: $H \rightarrow ZZ^* \rightarrow 4l$

arXiv:2004.03969



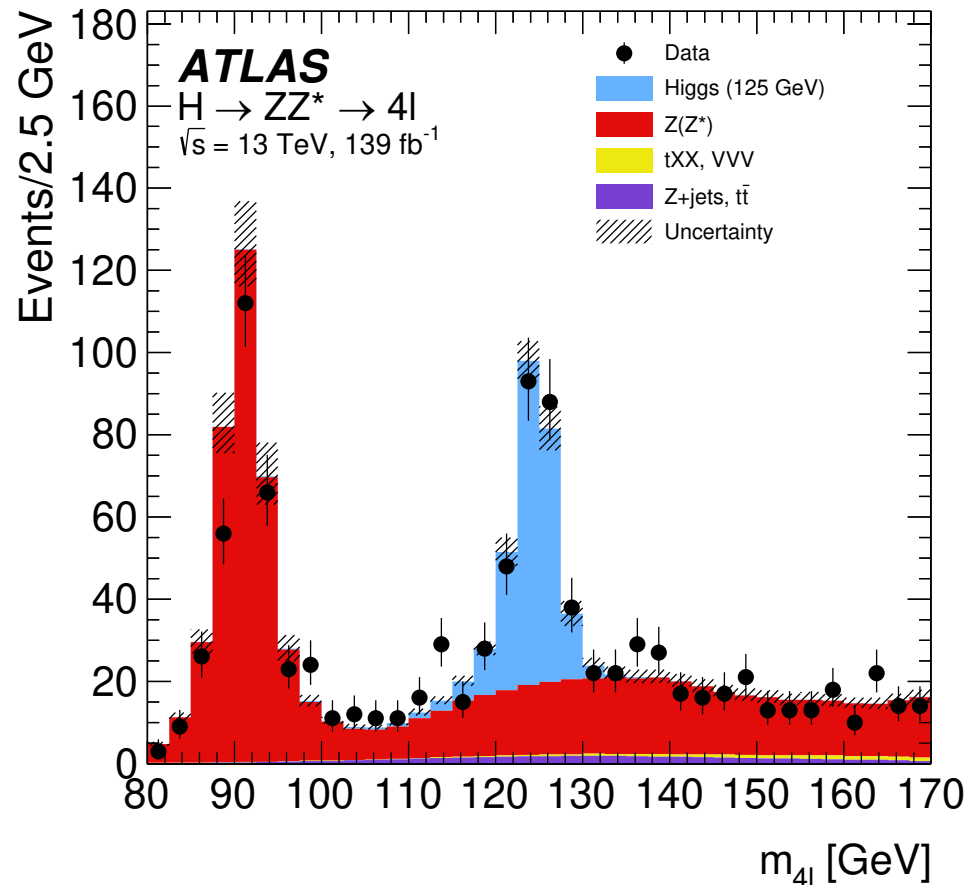
Low branching ratio: only 0.17% of all Higgs boson decays!

...but a very distinct signal,
and high purity in the Higgs
boson mass window:

Background from SM $Z(Z^*) \rightarrow 4l$
production: simulation constrained
by fitting regions outside the Higgs
boson mass window

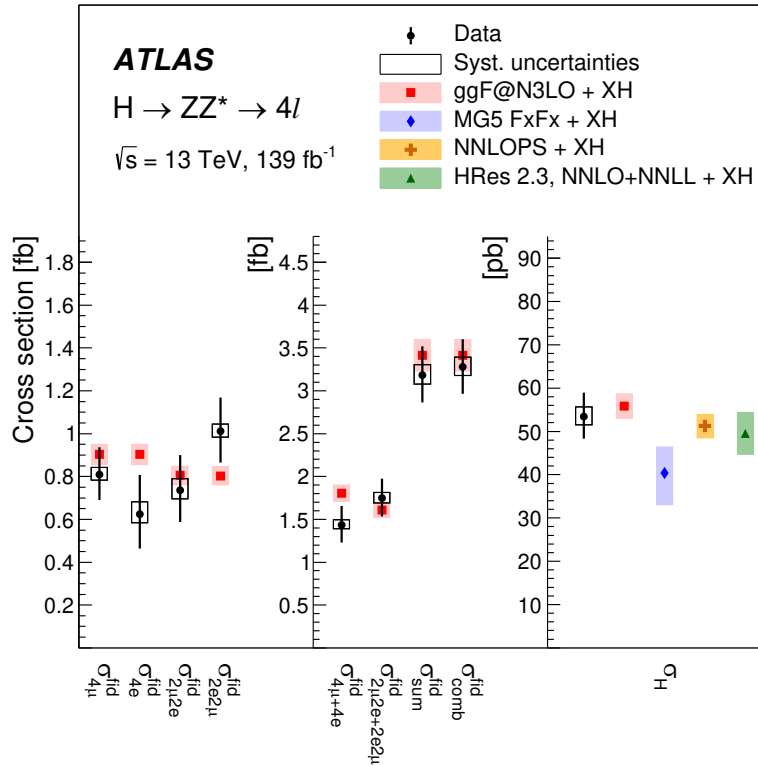
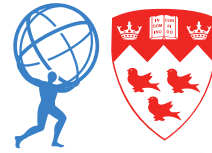
Multi-boson and tXX ($X=t, V$) are
estimated from simulation

Backgrounds from fake and non-
prompt leptons are measured
using a data-driven method



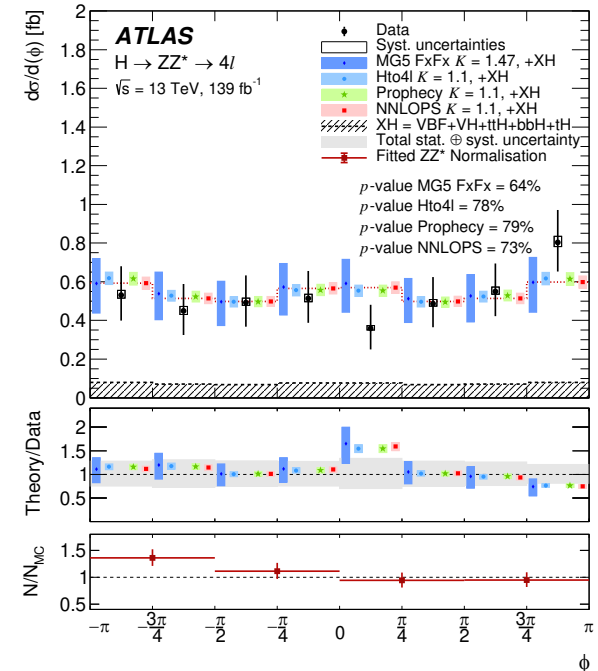
$H \rightarrow ZZ^* \rightarrow 4l$ cross sections

arXiv:2004.03969

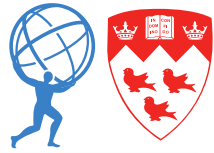


Unfolded, fiducial cross sections are measured for each channel and combined
 Inclusive Higgs boson production cross section σ_H measured using SM branching ratios
 → Overall good agreement with SM predictions

Differential cross sections for many variables, compared to different theoretical predictions, including jet-related variables and angular variables
 Showing here the azimuthal angle between the two Z bosons



Higgs boson mass: $H \rightarrow ZZ^* \rightarrow 4l$



CONF-2020-005

Improvements over the cross-section measurement:

FSR photons added to m_{4l} : 1% improvement in resolution

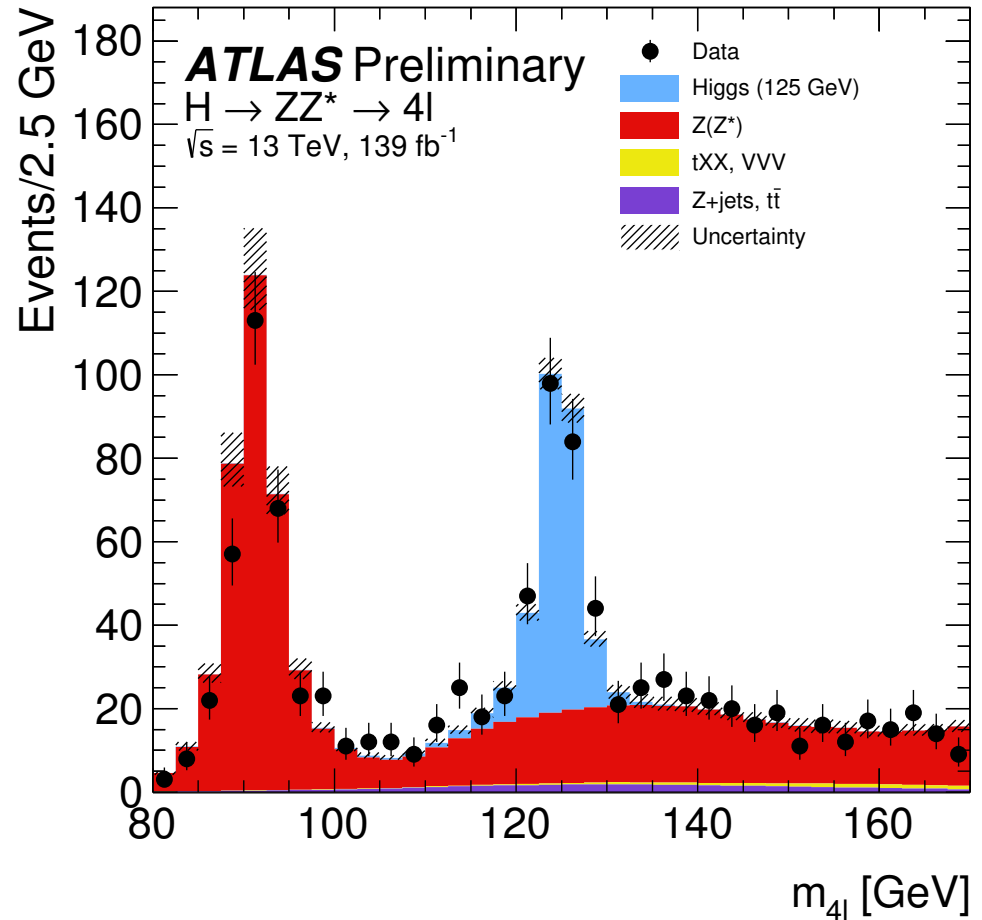
Kinematic fit used to constrain m_{12} to the Z boson mass: 17% improvement in resolution

Mass constraint:

$$115 < m_{4l} < 130 \text{ GeV}$$

316 ± 14 events, 66% signal

Signal lineshape dominated by detector response: m_{4l} distribution is modelled with a double-sided crystal ball distribution



Higgs boson mass: $H \rightarrow ZZ^* \rightarrow 4l$

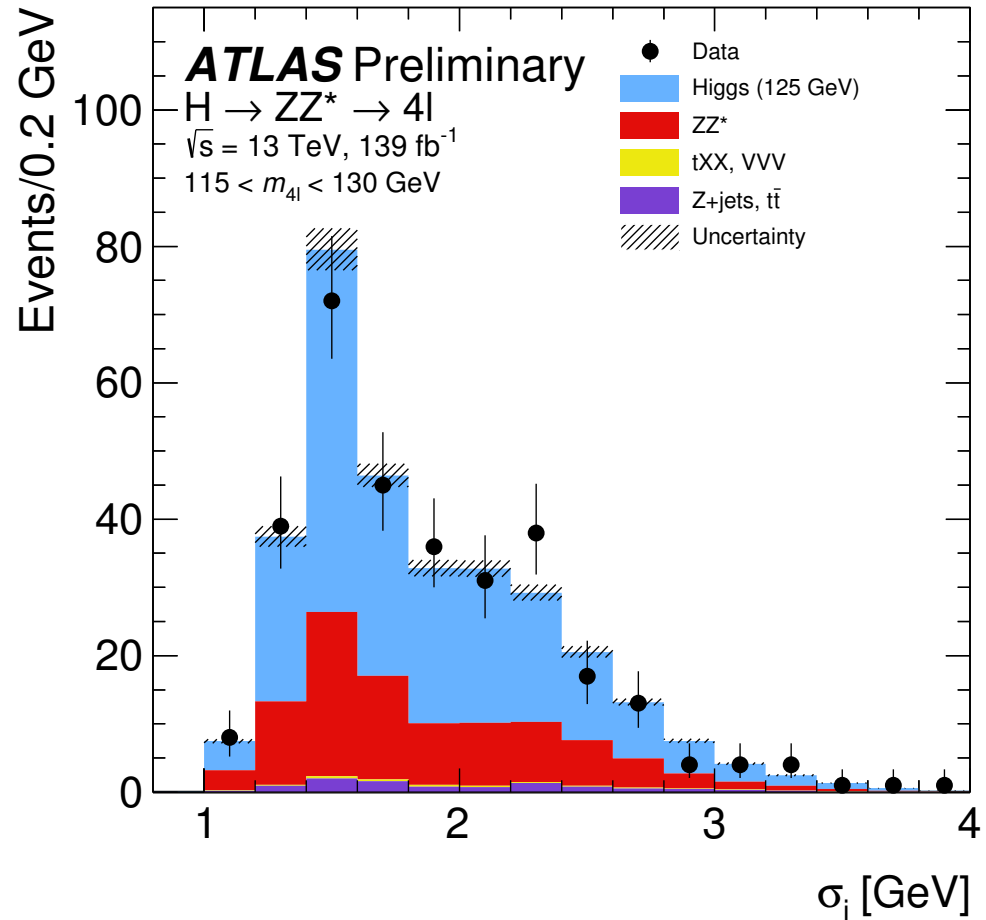


CONF-2020-005

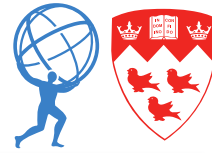
Use the event-level resolution σ_i instead of the average resolution σ in the fit

Estimate σ_i using a quantile regression neural network:

Input individual lepton kinematics and the four-lepton momentum and its uncertainty

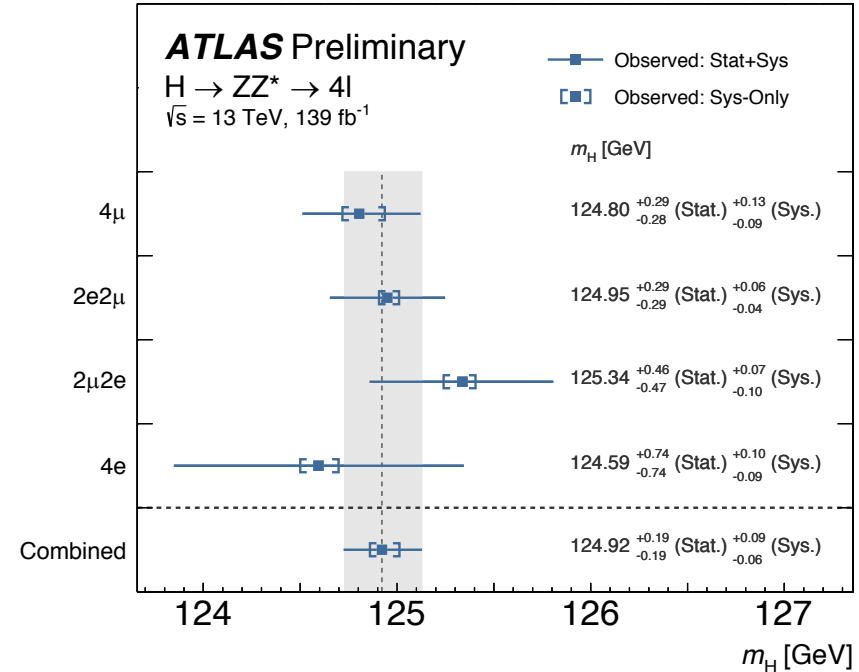
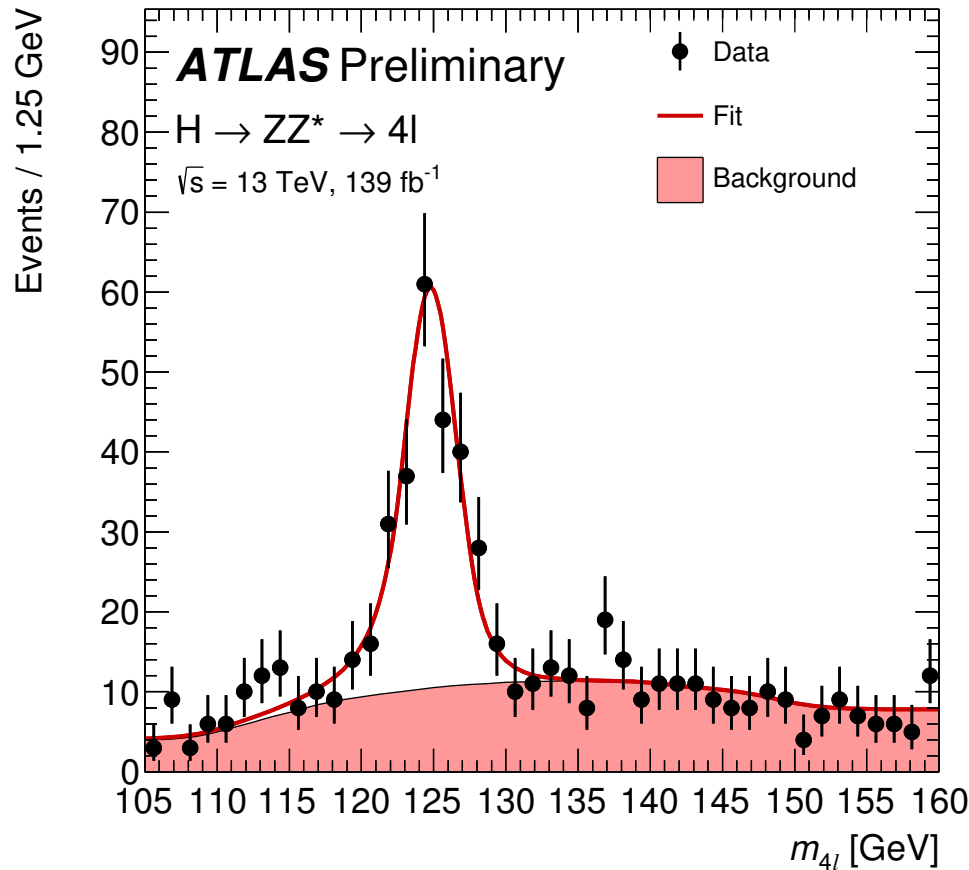


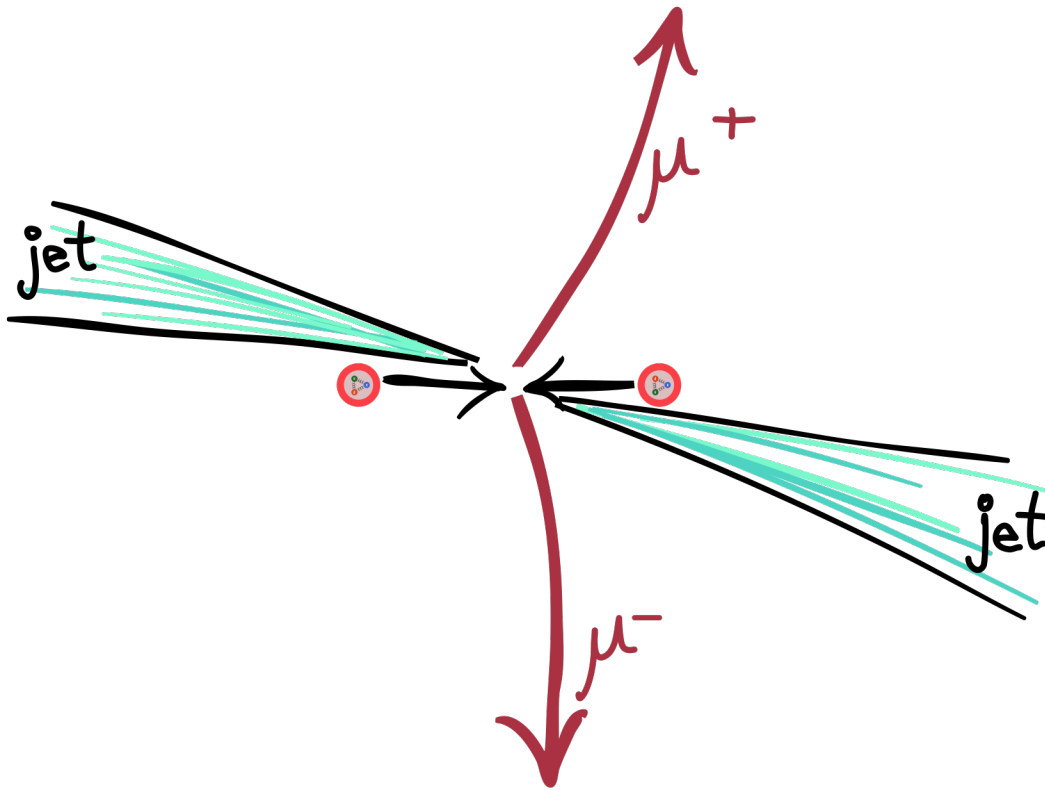
Higgs boson mass: $H \rightarrow ZZ^* \rightarrow 4l$



CONF-2020-005

Measured $m_H = 124.92^{+0.19}_{-0.19}$ (Stat.) $^{+0.09}_{-0.06}$ (Sys.) GeV





Electroweak Z_{jj} production

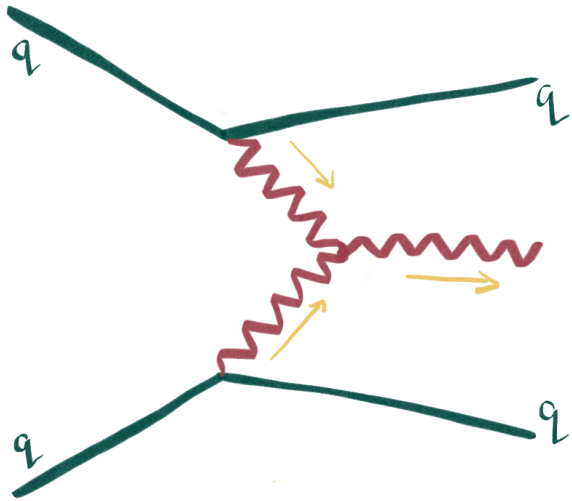
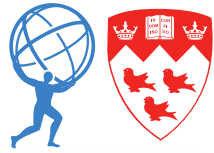
Z boson decaying
leptonically ($2e/2\mu$)

Two jets

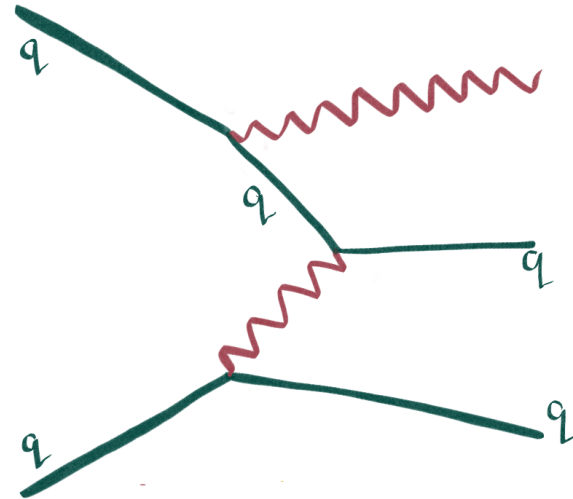
- Large rapidity separation
- Large invariant mass

No jets in the gap

Electroweak Z_{ij} production



vector boson fusion
 $\mathcal{O}(\alpha_{EW}) = 3$

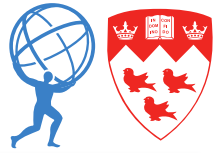


Z_{ij} production
 $\mathcal{O}(\alpha_{EW}) = 3$

We cannot directly measure vector boson fusion – there is **significant interference** with other diagrams of the same order in α_{EW} , and extracting the VBF component is not a gauge invariant operation

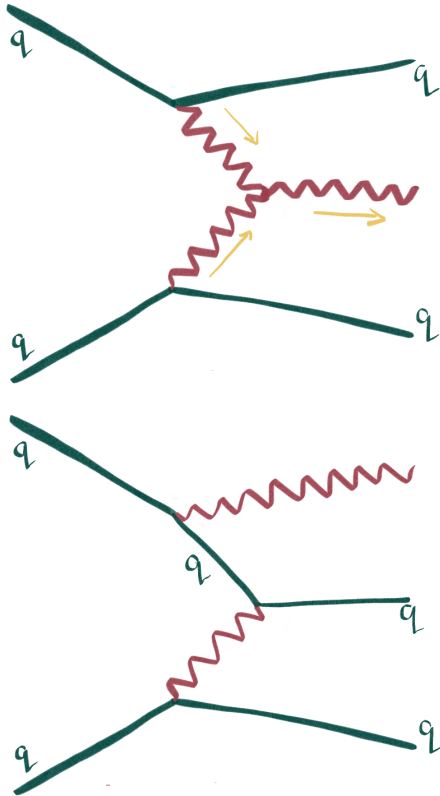
→ Measure electroweak production of Z_{ij}

Electroweak Z_{jj} production



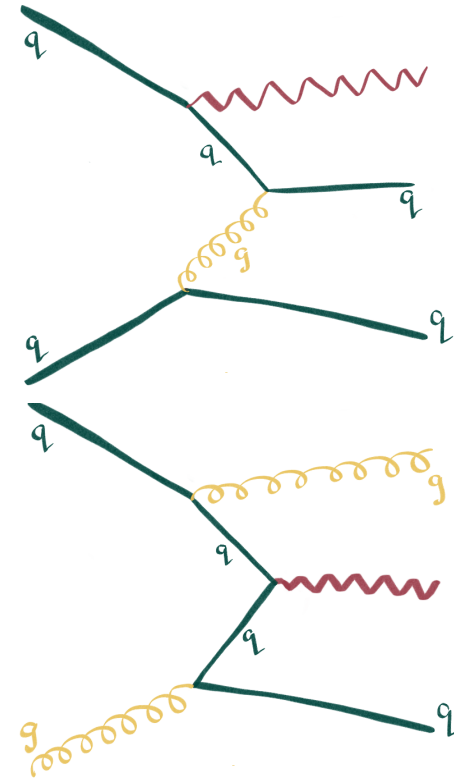
Electroweak V_{jj} production

$$\mathcal{O}(\alpha_{EW}) = 3$$



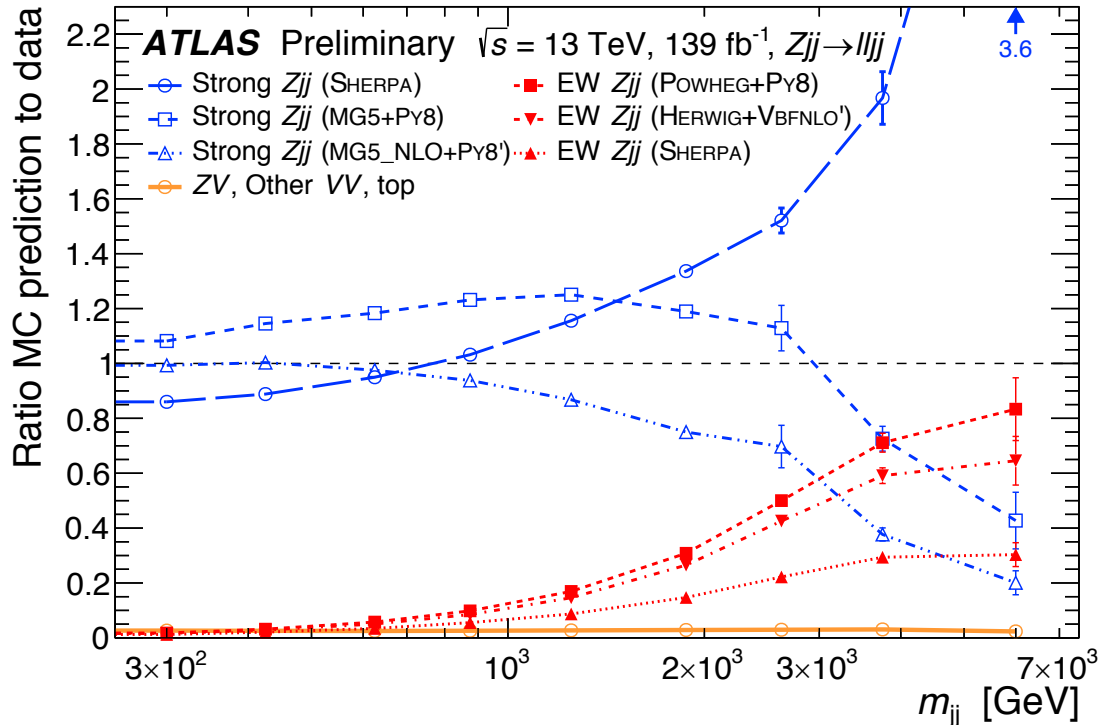
Strong V_{jj} production

$$\mathcal{O}(\alpha_{EW}) = 1, \mathcal{O}(\alpha_S) = 2$$



Strong production has the **same final state** and a **higher cross-section**

Electroweak Z_{jj} production



Strong Z_{jj} is the largest background across the spectrum

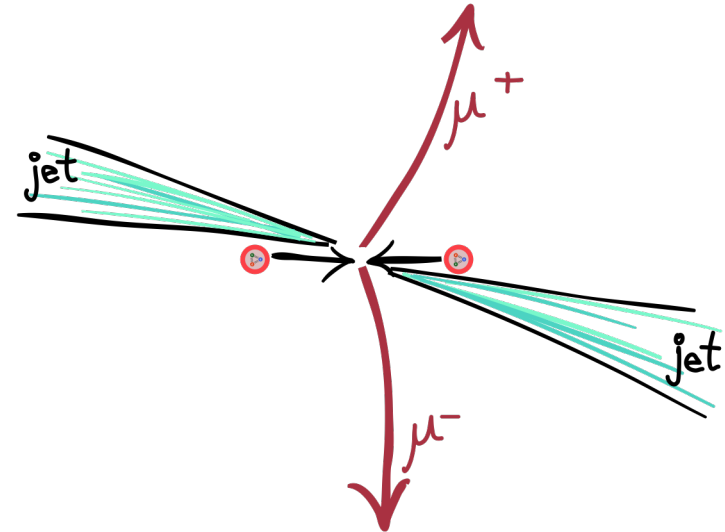
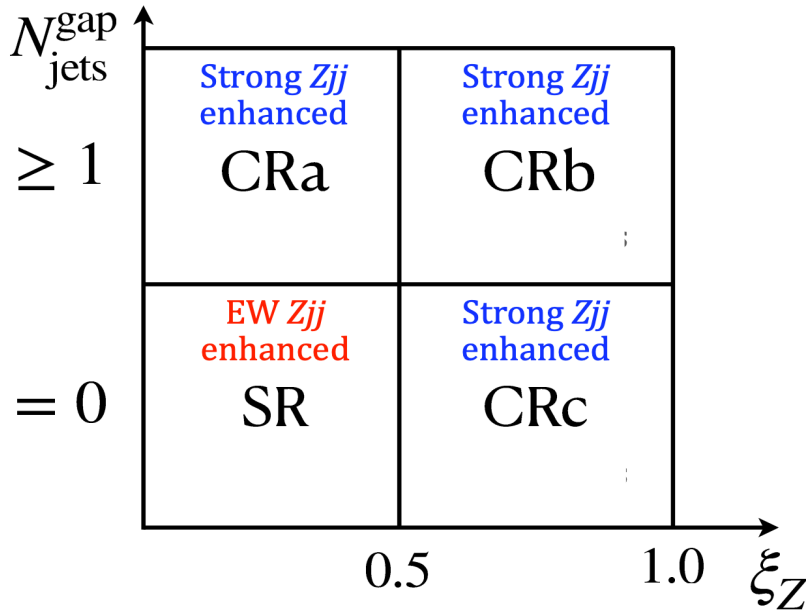
Monte Carlo modelling of both strong electroweak Z_{jj} shows discrepancies between generators

Modelling of strong Z_{jj} is especially poor, particularly in the high- m_{jj} signal-enriched region

Data-driven background modelling



CERN-EP-2020-045



Analysis is split into four regions with two uncorrelated variables:

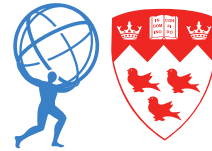
number of jets **between** the leading and subleading jets

centrality of the reconstructed Z boson:

$$\xi_Z = |y_{\ell\ell} - 0.5(y_{j1} + y_{j2})| / |\Delta y_{jj}|$$

→ three background-enhanced regions and one signal region fit to reduce dependence on mismodelling

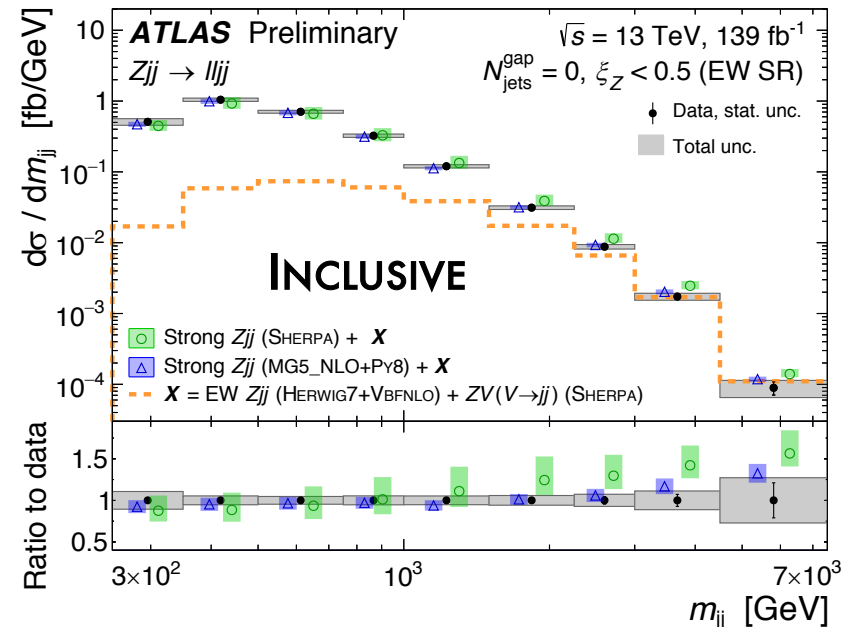
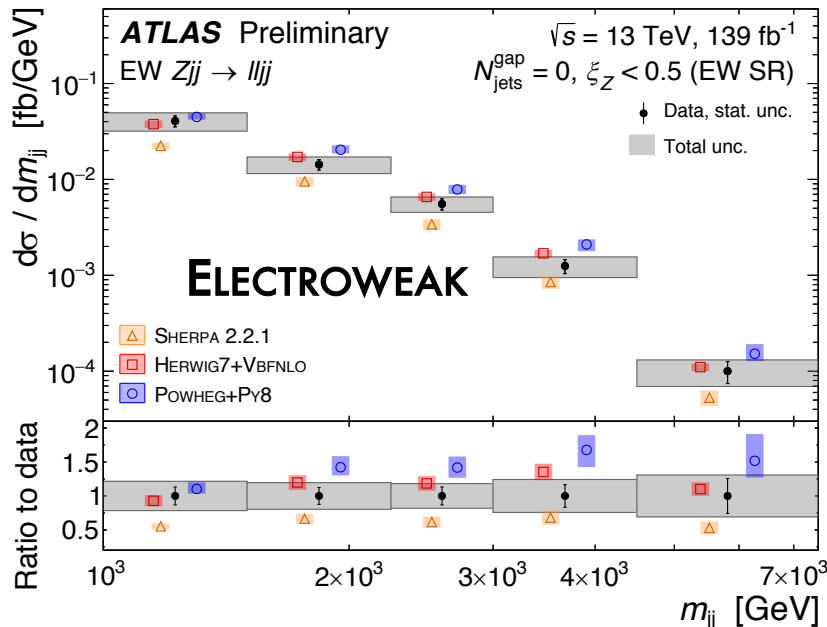
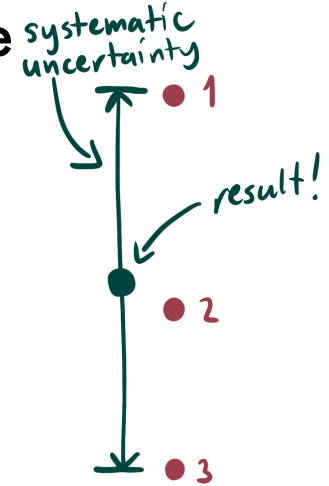
Results



Extract the electroweak Z_{ij} signal once for each of the three strong Z_{ij} MC generators:

result is the midpoint of the envelope

Signal and control regions are unfolded for both electroweak and inclusive Z_{ij} yields:

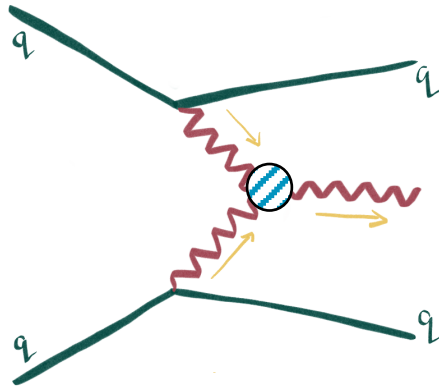


Effective field theory interpretation



CERN-EP-2020-045

$$\sigma_{EFT} = \sigma_{SM} + \sum \frac{c_j}{\Lambda^3} \sigma_{SM,j}^{interf.} + \sum_j \frac{c_j^2}{\Lambda^6} \sigma_j^{NP} + \sum_{j \neq k} \frac{c_j c_k}{\Lambda^6} \sigma_{jk}^{NP - interf.}$$

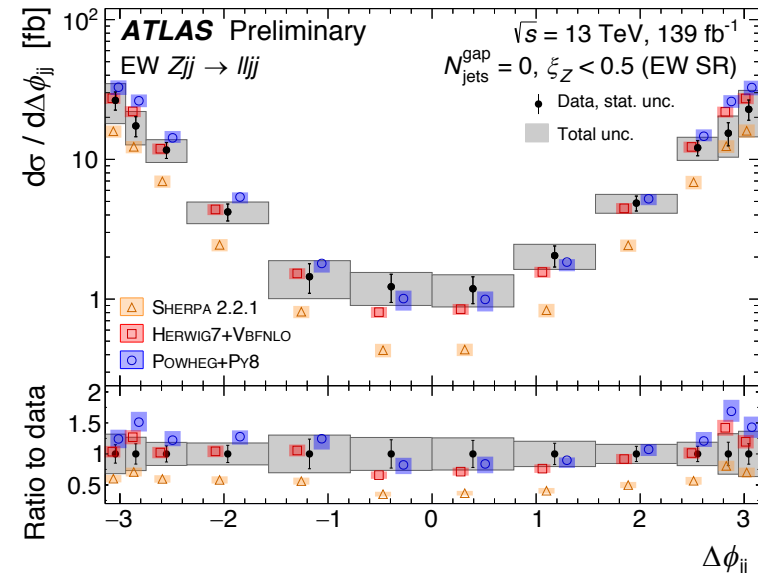


Wilson coefficient	Linear EFT	95 % confidence limit [TeV ⁻²]	
		Expected (Asimov)	Observed
c_W/Λ^2	yes	[-0.30, 0.30]	[-0.19, 0.41]
	no	[-0.31, 0.29]	[-0.19, 0.41]
\tilde{c}_W/Λ^2	yes	[-0.12, 0.12]	[-0.11, 0.14]
	no	[-0.12, 0.12]	[-0.11, 0.14]
c_{HWB}/Λ^2	yes	[-2.45, 2.45]	[-3.78, 1.13]
	no	[-3.11, 2.10]	[-6.31, 1.01]
$\tilde{c}_{HWB}/\Lambda^2$	yes	[-1.06, 1.06]	[0.23, 2.34]
	no	[-1.06, 1.06]	[0.23, 2.35]

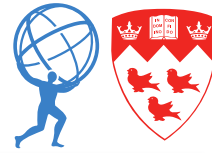
Two CP-even and two CP-odd operators were tested

→ sensitivity to CP-odd operators through the parity-odd observable

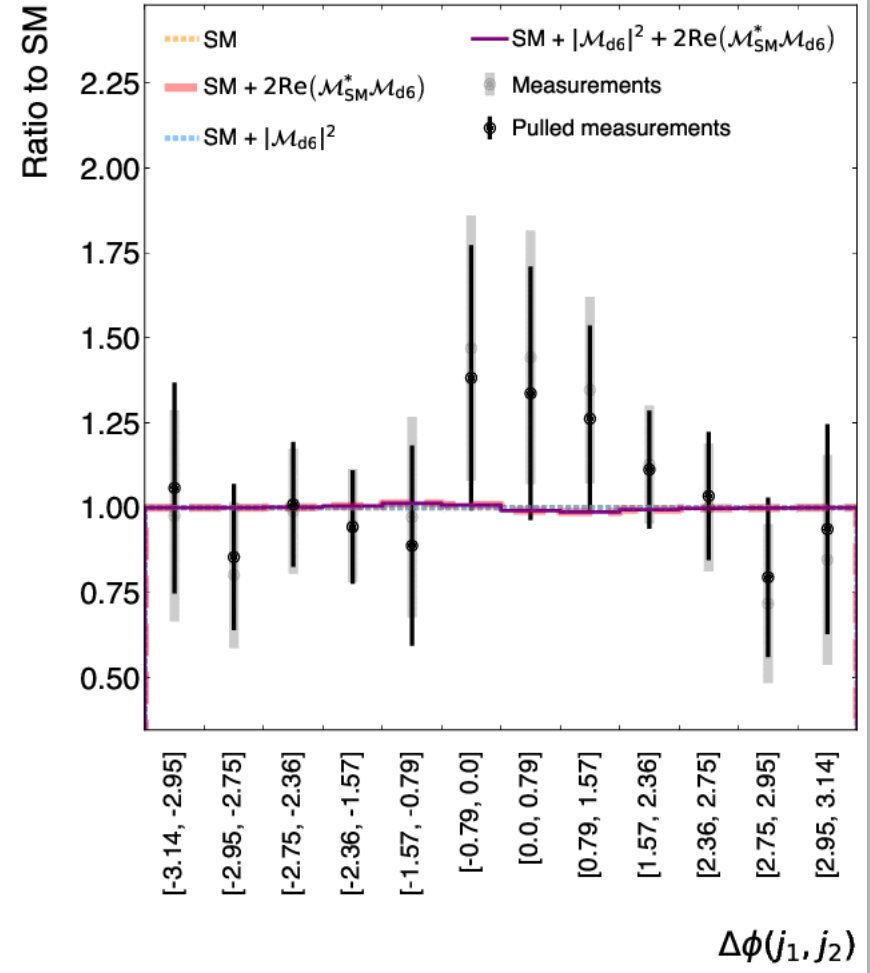
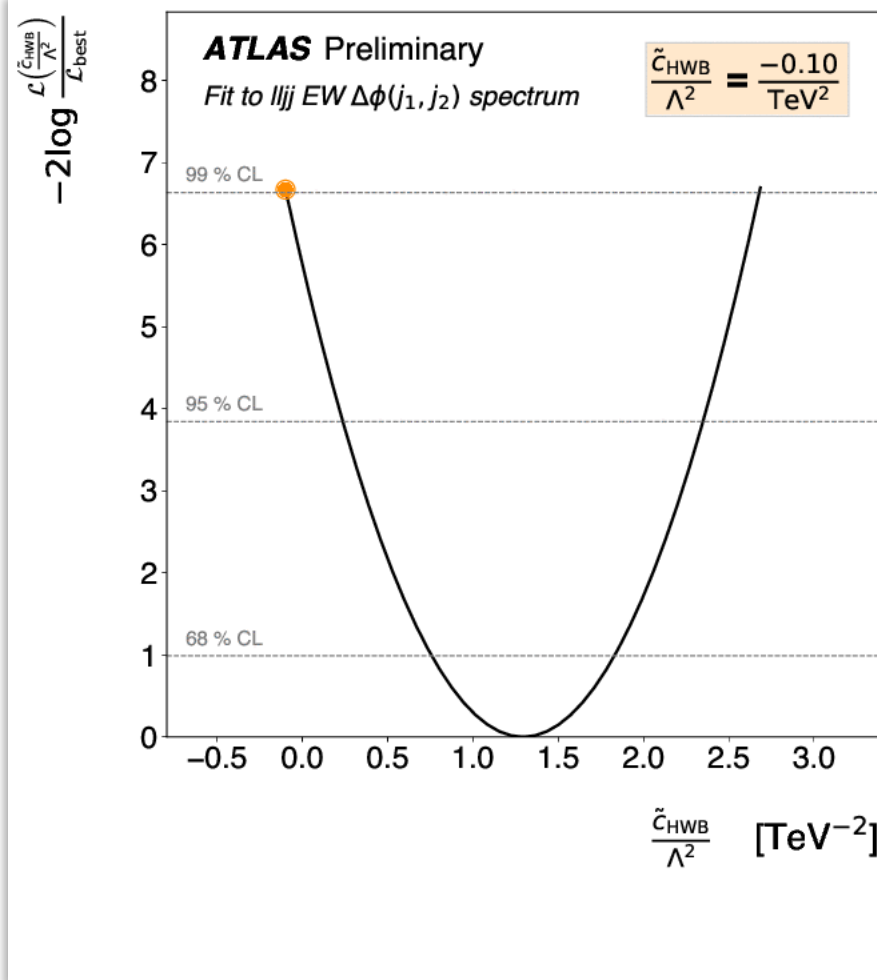
$\Delta\phi_{jj} = \phi_{\text{higher rapidity jet}} - \phi_{\text{lower rapidity jet}}$
 where jj = the two leading jets



Effective field theory interpretation



CERN-EP-2020-045

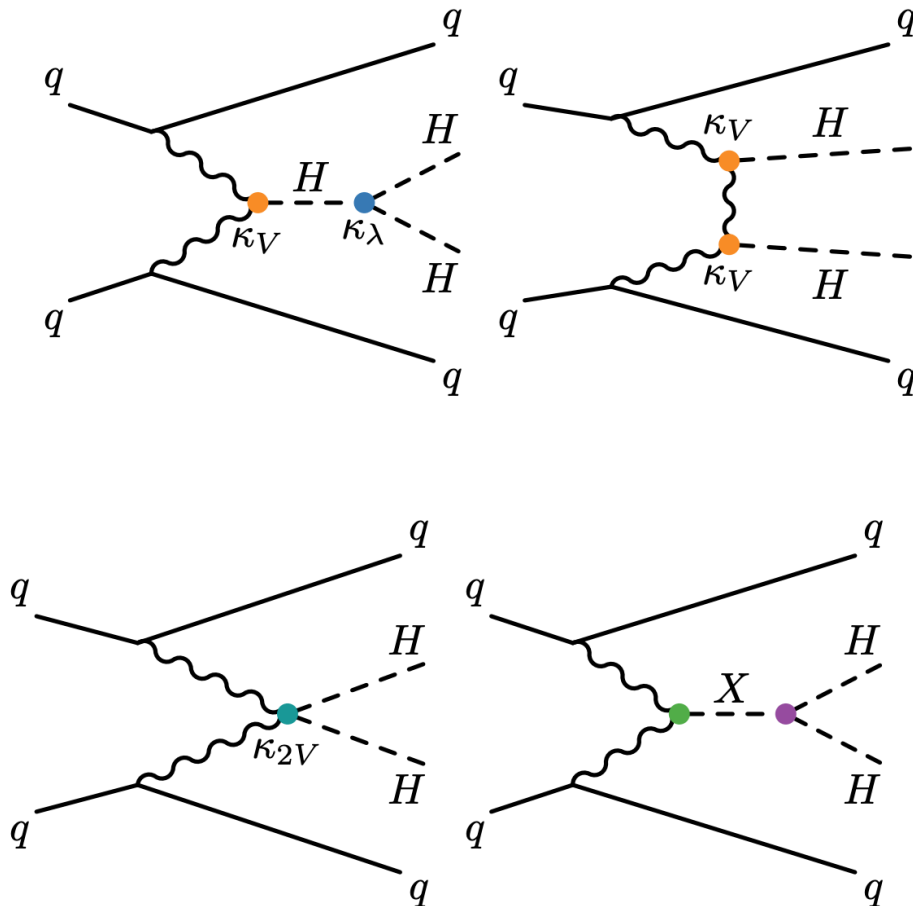


VBF di-Higgs searches

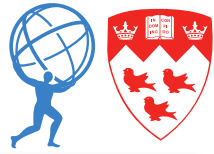
Four central b -tagged jets

Two jets

- Large rapidity separation
- Opposite sides of the detector
- Large invariant mass

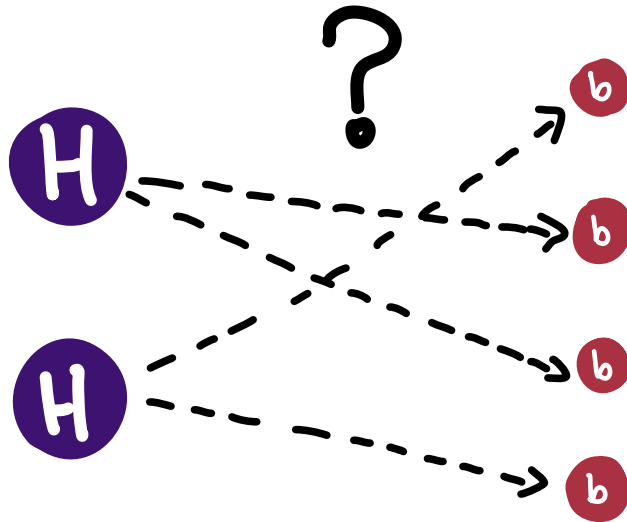


VBF di-Higgs – finding the Higgs



arXiv:2001.05178

Two Higgs bosons decay into four b -jets:



Exactly 4 b -tagged jets with $p_T > 40$, $ \eta < 2.0$	
If $m_{4b} < 1250$	$\frac{360}{m_{4b}} - 0.5 < \Delta R_{bb}^{\text{lead}} < \frac{653}{m_{4b}} + 0.475$ $\frac{235}{m_{4b}} < \Delta R_{bb}^{\text{subl}} < \frac{875}{m_{4b}} + 0.35$
If $m_{4b} \geq 1250$	$\Delta R_{bb}^{\text{lead}} < 1$ $\Delta R_{bb}^{\text{subl}} < 1$
Pairs with minimum	
$D_{HH} = \sqrt{(m_{2b}^{\text{lead}})^2 + (m_{2b}^{\text{subl}})^2} \left \sin \left(\tan^{-1} \left(\frac{m_{2b}^{\text{subl}}}{m_{2b}^{\text{lead}}} \right) - \tan^{-1} \left(\frac{116.5}{123.7} \right) \right) \right $	

Criteria based on **pairs of b -jets**, forming **Higgs boson candidates**

Pair of pairs with **minimum D_{HH}** is chosen:

correct 83% of the time for SM non-resonant HH

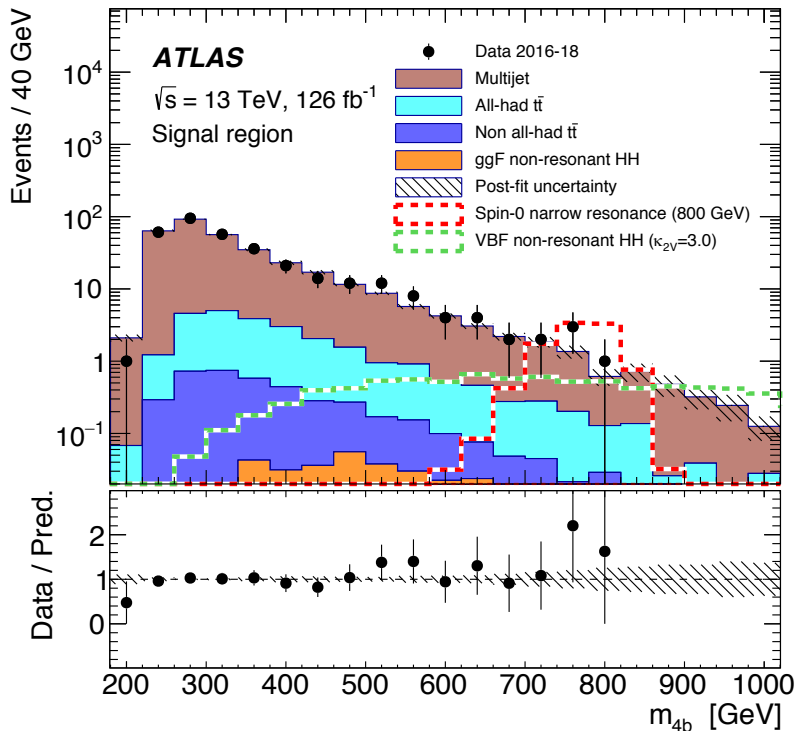
correct 91% of the time for broad BSM resonance \rightarrow HH

VBF di-Higgs – results

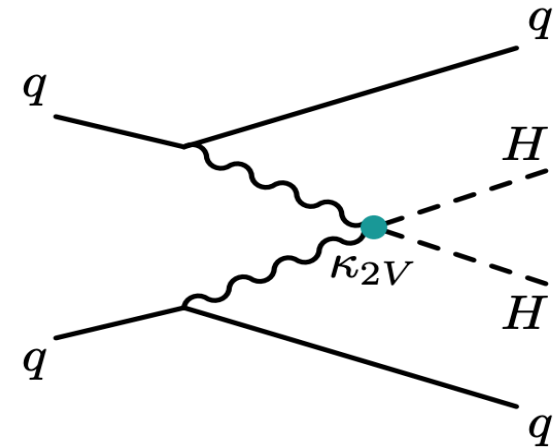
arXiv:2001.05178



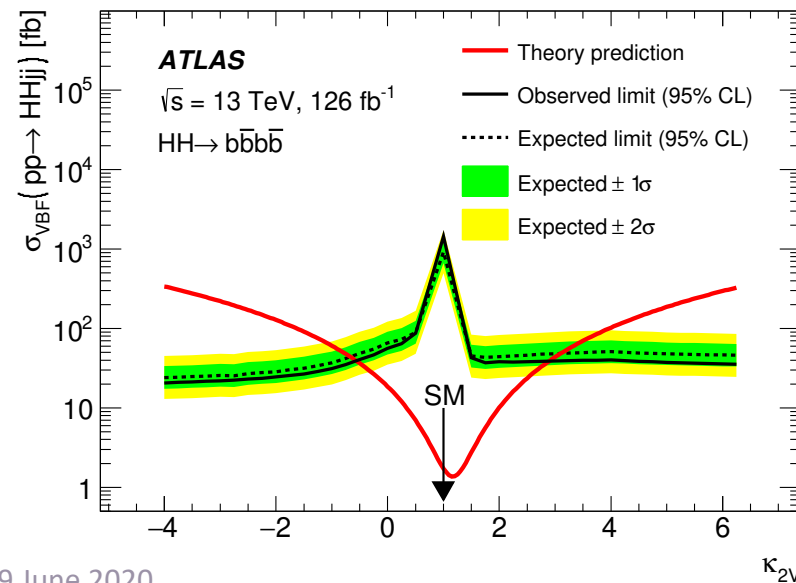
Observed 95% CL upper limit of 1450 fb on SM VBF HH production ($\sigma_{SM} = 1.73$ fb)



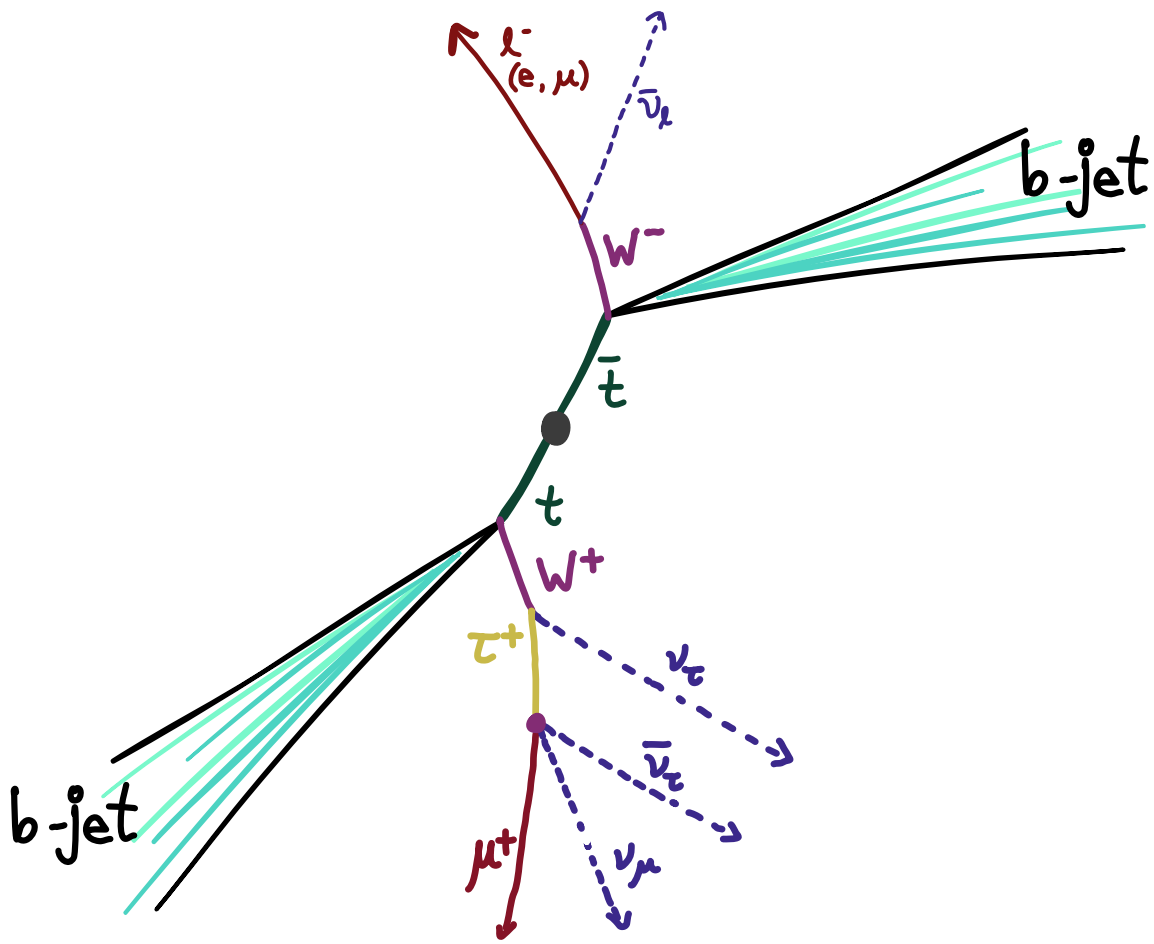
Not shown: limits also set on narrow and broad BSM $X \rightarrow HH$ resonances



Sensitivity to HHVV coupling (κ_{2V}) unique to VBF HH searches



Tag the event



Probe what happens here!

Universality of lepton couplings in W boson decays

- tt events: two b-jets
- One leptonically decaying W (e/μ) as a tag
- Second opposite-sign leptonically decaying W (μν or τν → μννν)
- Z mass veto

LFU in W boson decays

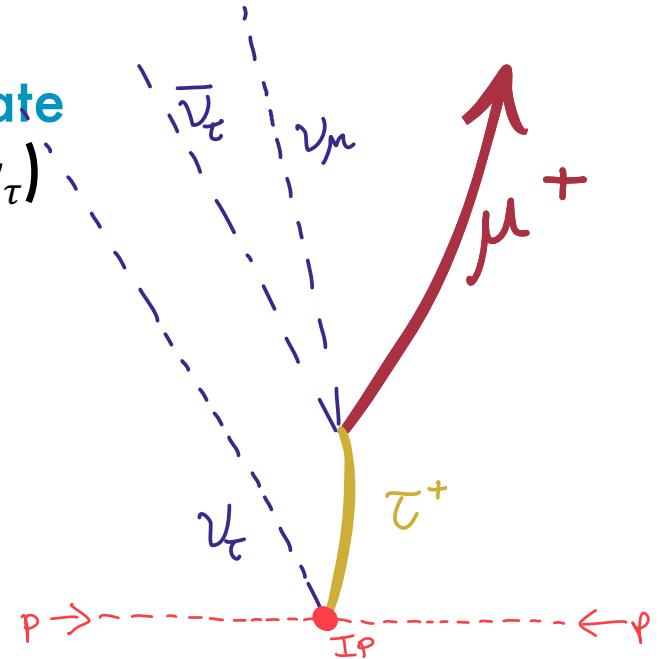
In the SM, gauge boson decays exhibit **lepton flavour universality**

Measure the **ratio of tau decays to muon decays**: Only previous measurement is from LEP, which shows a 2.7σ discrepancy from the SM

$$R(\tau/\mu) = \frac{\text{BR}(W \rightarrow \tau\nu)}{\text{BR}(W \rightarrow \mu\nu)}$$

Use $\tau \rightarrow \mu$ decays to have the **muon final state** for both lepton flavours ($W \rightarrow \tau\nu_\tau \rightarrow \mu\nu_\mu\nu_\tau\nu_\tau$)

Properties of muons from $W \rightarrow \mu\nu$ vs. $W \rightarrow \tau\nu$ differ: form templates for each decay channel and fit to data

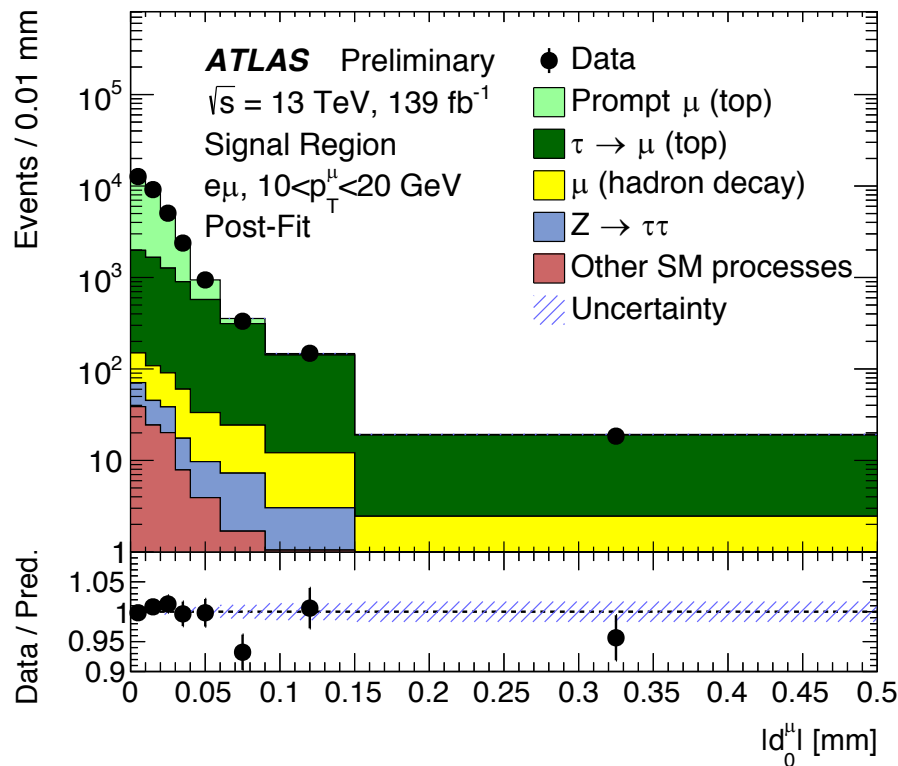


LFU in W boson decays

48-bin fit (3 muon p_T bins, 8 muon d_0 bins, two tag-lepton channels) to extract two parameters:

$R(\tau/\mu)$: parameter of interest, applied to $\tau \rightarrow \mu$ (top) component

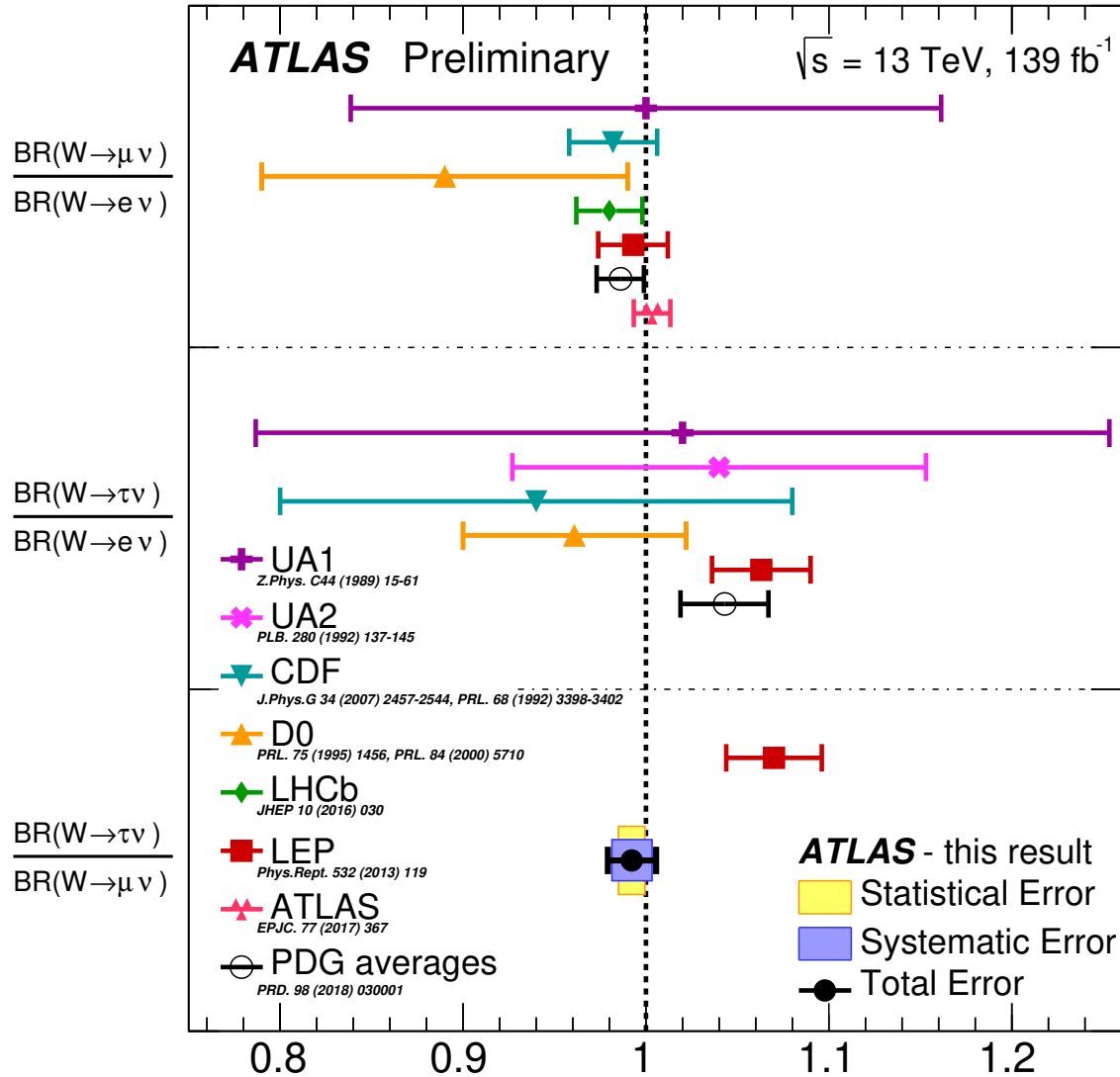
$k(tt)$: normalization applied to both tt and Wt

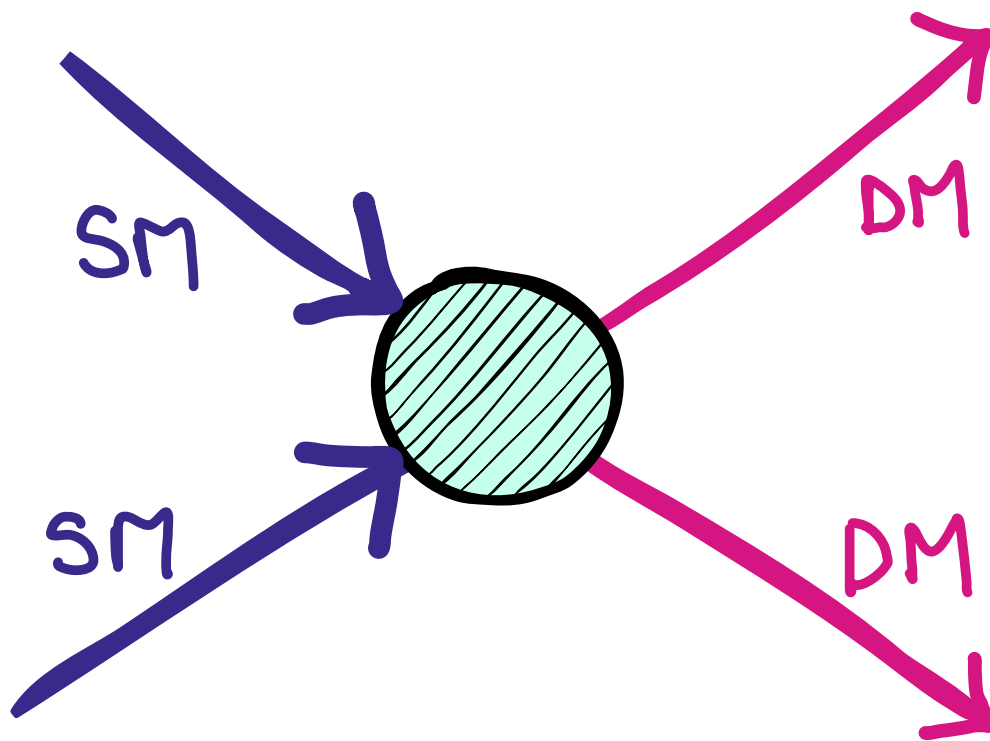


$$R(\tau/\mu) = 0.992 \pm 0.013$$
$$[\pm 0.007 \text{ (stat)} \pm 0.011 \text{ (syst)}]$$

Most precise value to-date!

LFU in W boson decays



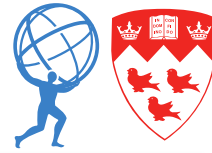


Searches for Dark Matter

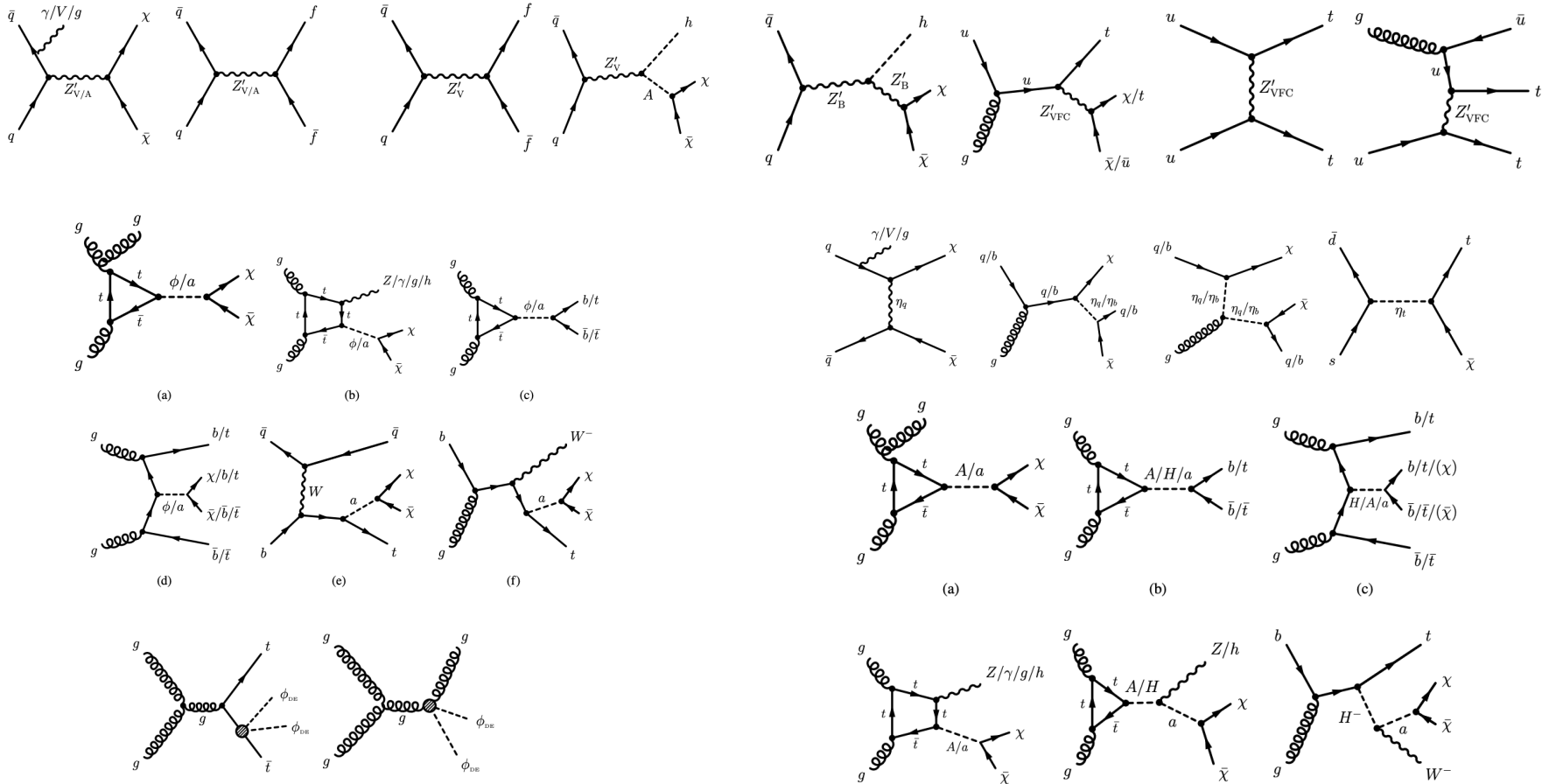
•————•

Many, many possibilities!

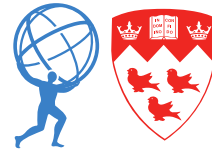
Dark matter summary



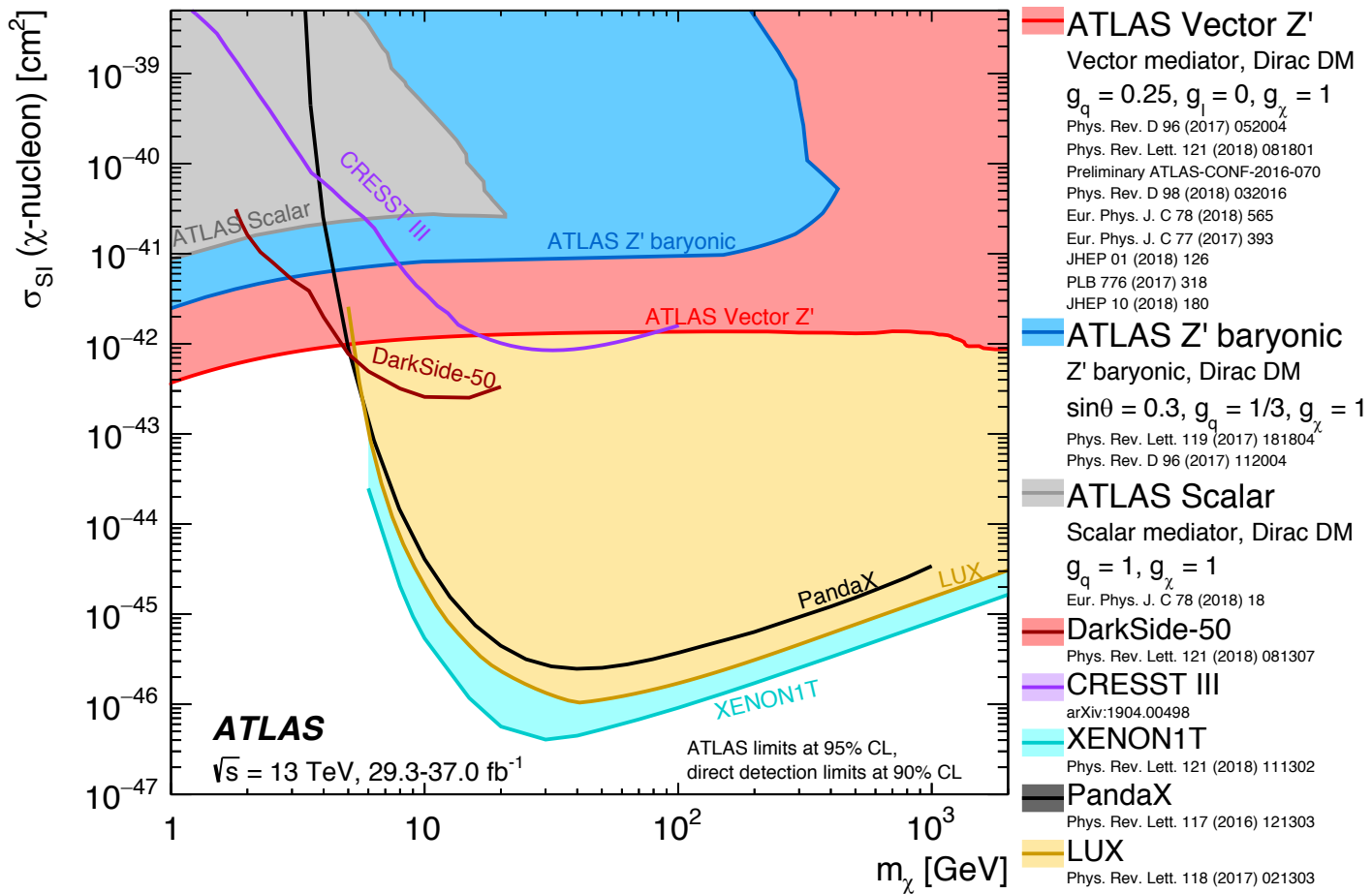
Dark matter could be produced in many, many ways at the LHC:



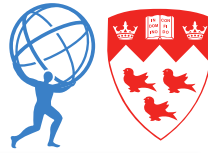
Dark matter summary



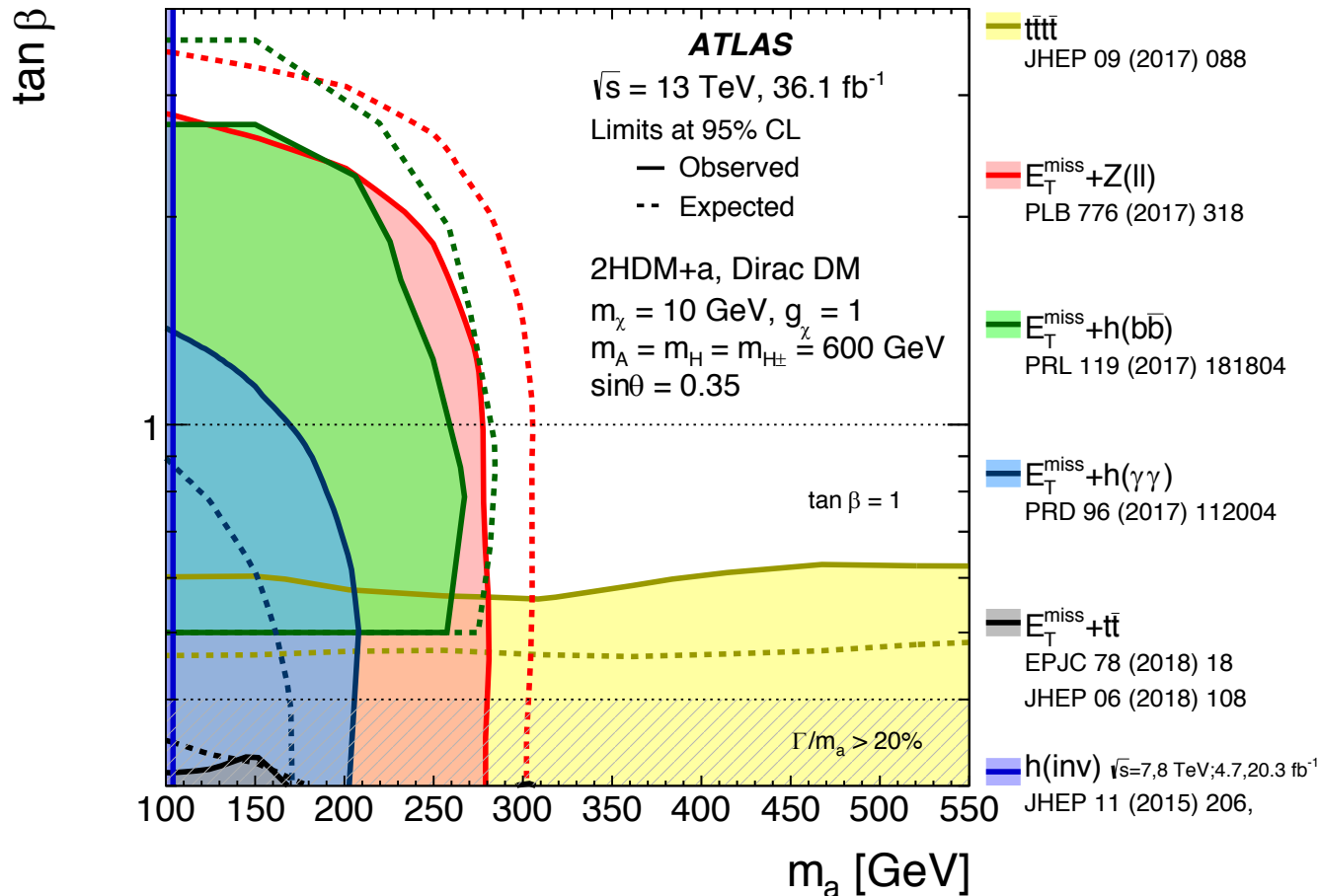
Important to understand how ATLAS compare to other experiments:



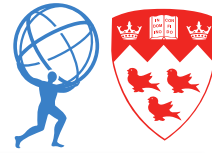
Dark matter summary



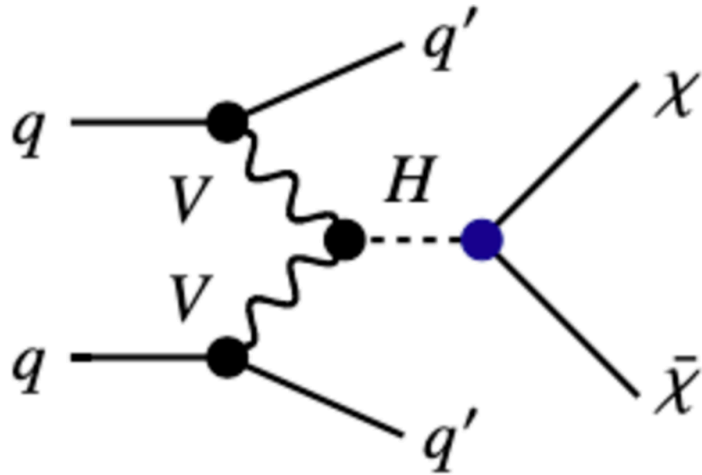
Important to understand how searches in different channels are complementary, and what areas of phase space we still need to focus on:



DM in invisible Higgs boson decays



CONF-2020-008



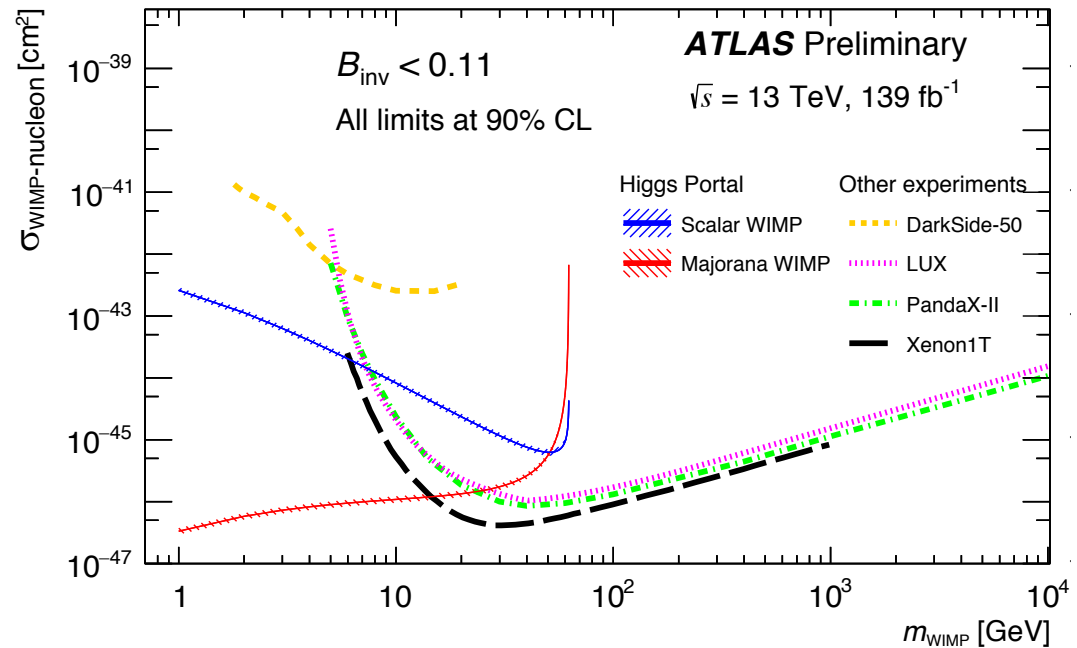
In the SM, the Higgs boson decays invisibly 0.12% of the time

Previous best fit measurement:

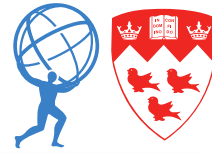
$< 26\%$ at 95% CL [PRL 122, 231801 \(2019\)](#)

Full Run 2 preliminary result has limited this to $< 13\%$ at 95% CL!

Strong $BR_{\text{invisibles}}$ limit can be interpreted as strong constraints on Higgs portal DM:



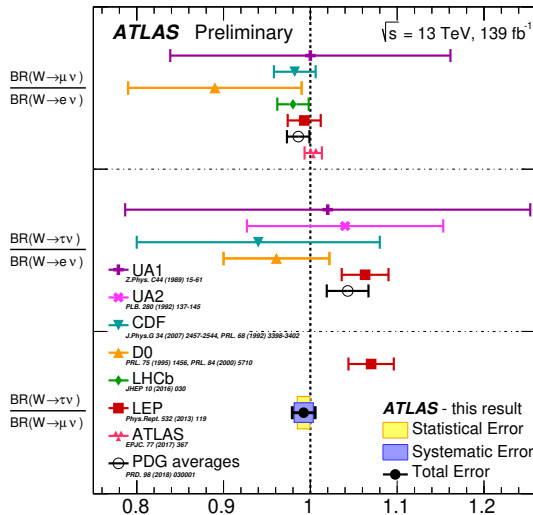
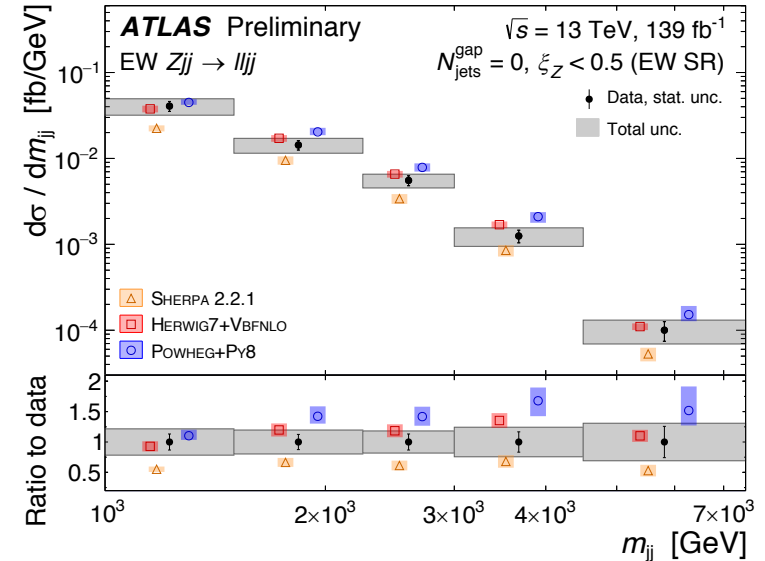
Summary



CERN-EP-2020-045

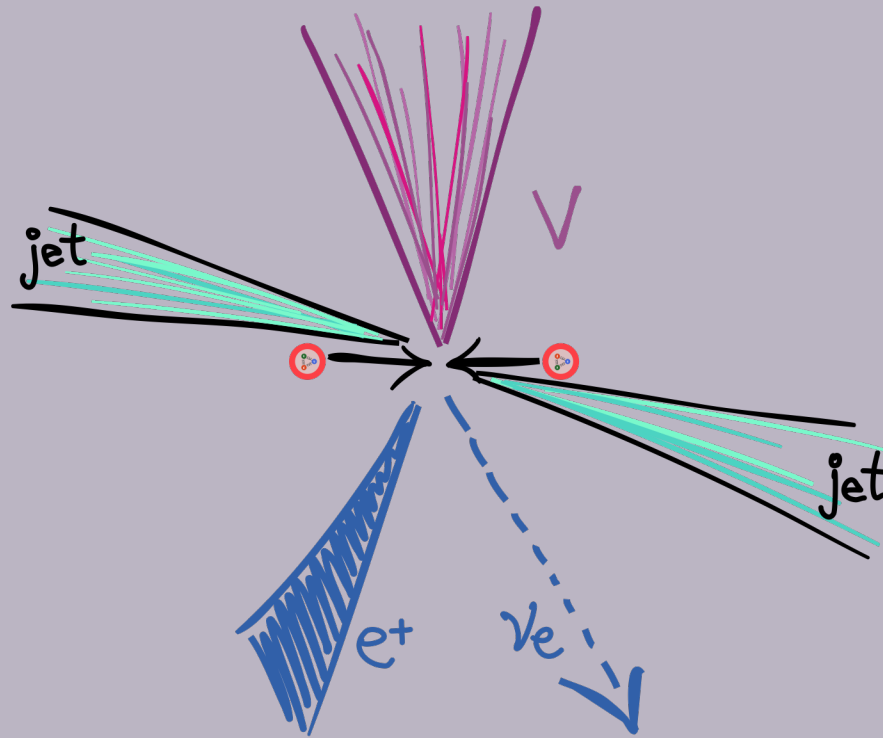
ATLAS has a hugely diverse physics program

Many results using the full Run 2 dataset are already complete



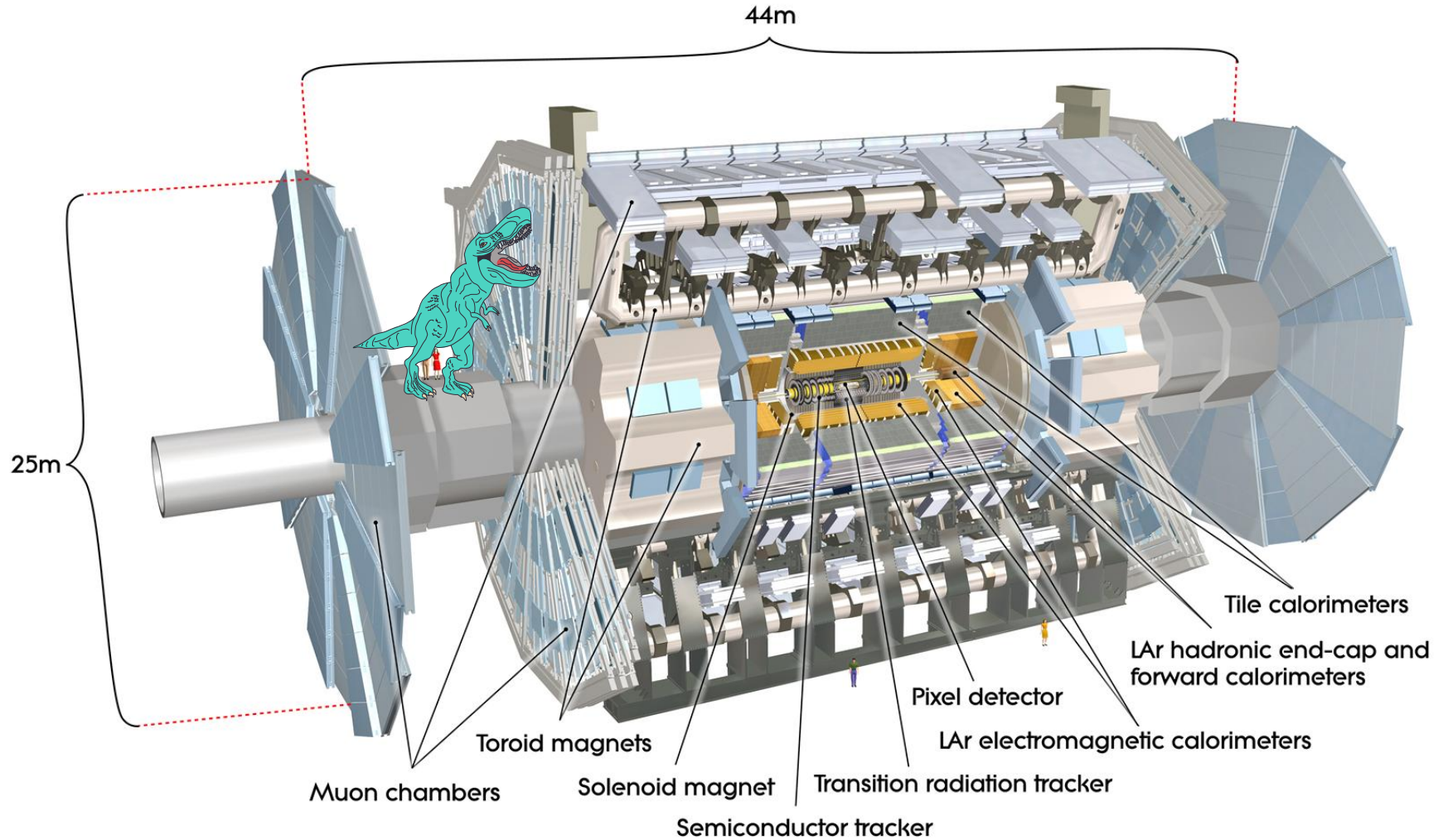
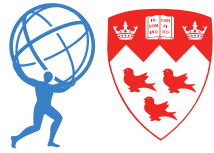
I've only shown a small handful of what we have:
 Higgs $\rightarrow ZZ^* \rightarrow 4l$
 VBF HH
 VBF Z
 R(tau/mu) in W decays
 Dark matter searches

...and many more interesting results are still to come!

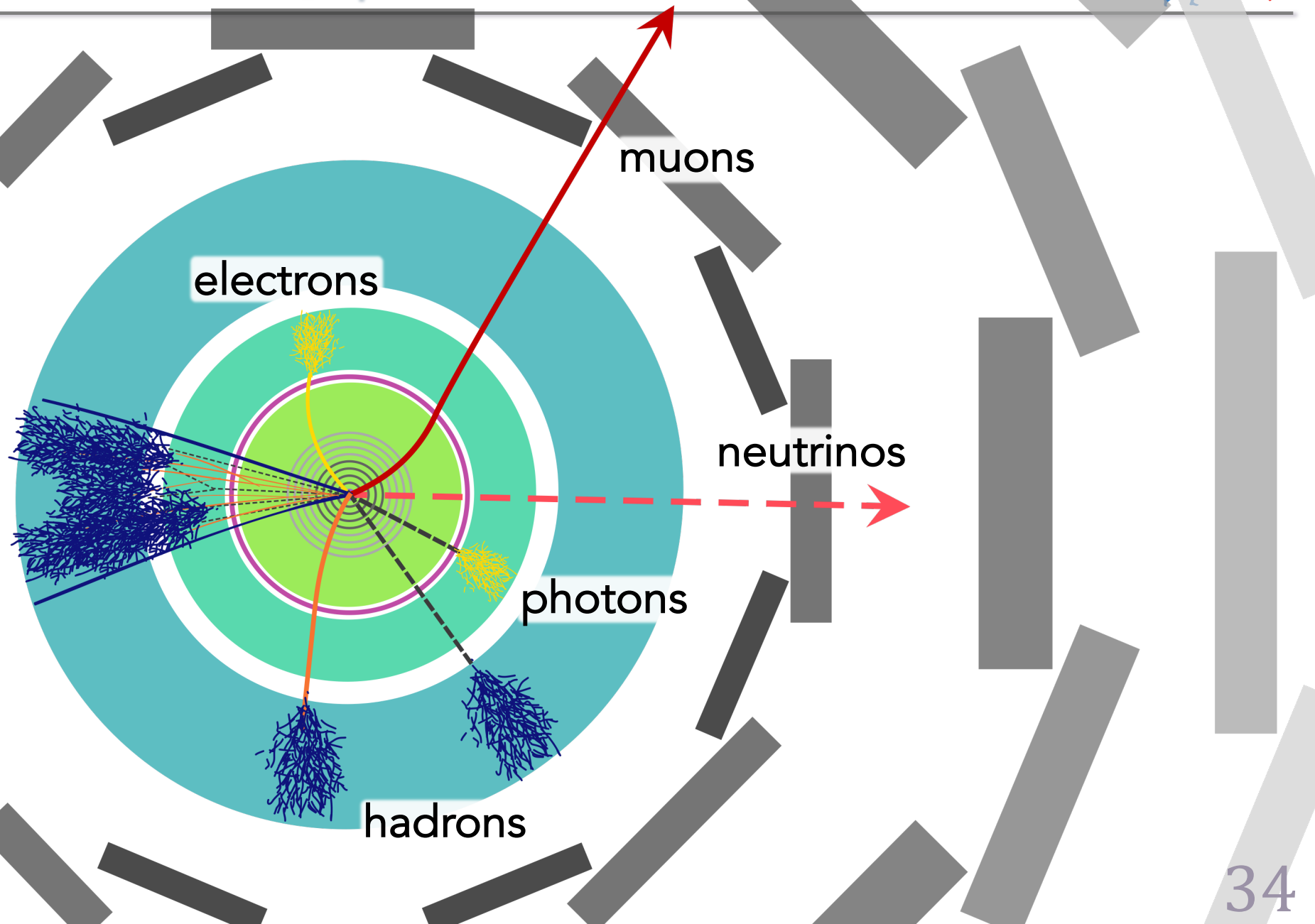


Backup

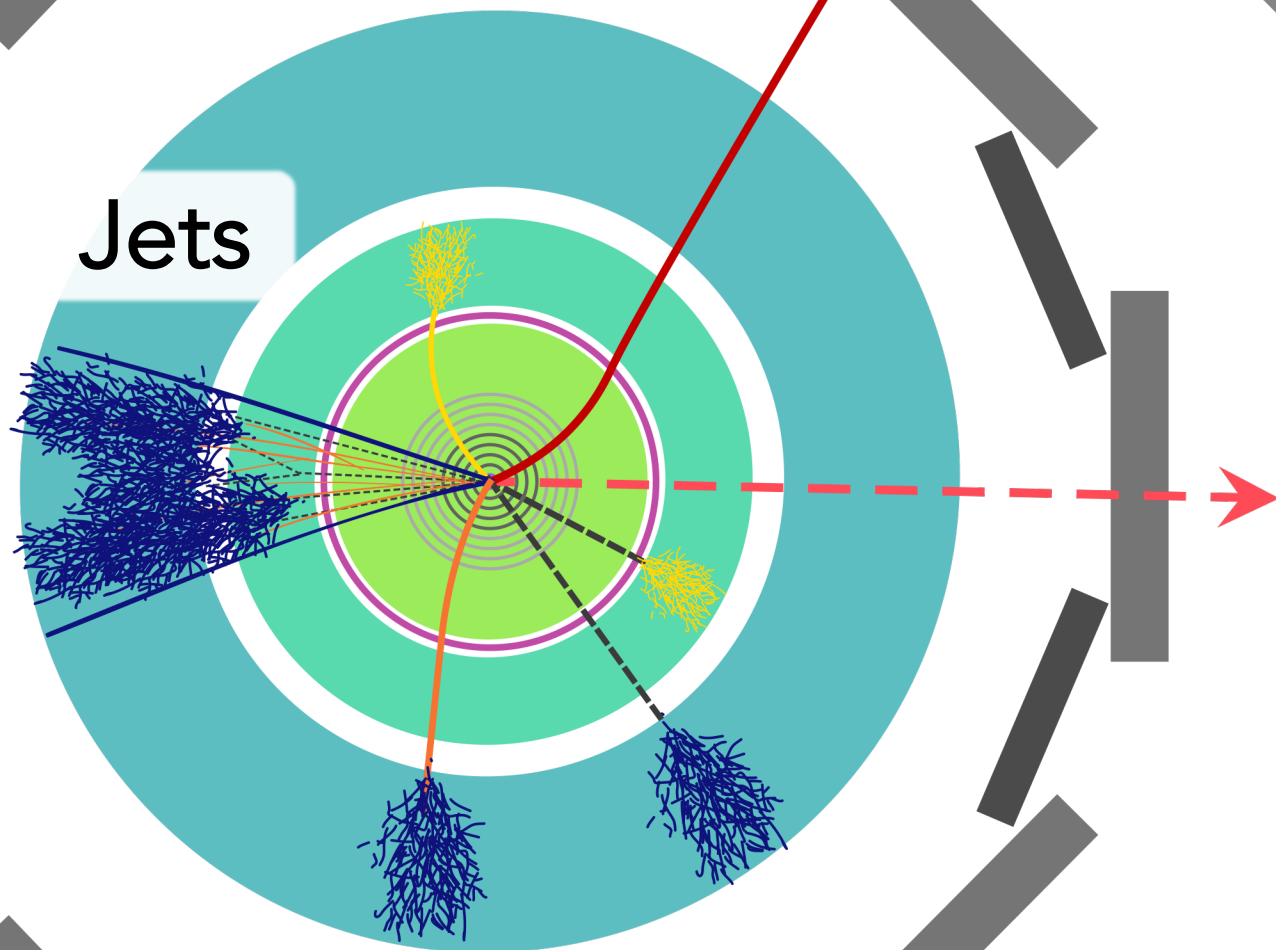
The ATLAS detector



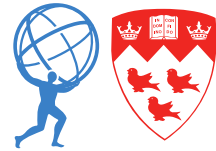
Detecting particles with ATLAS



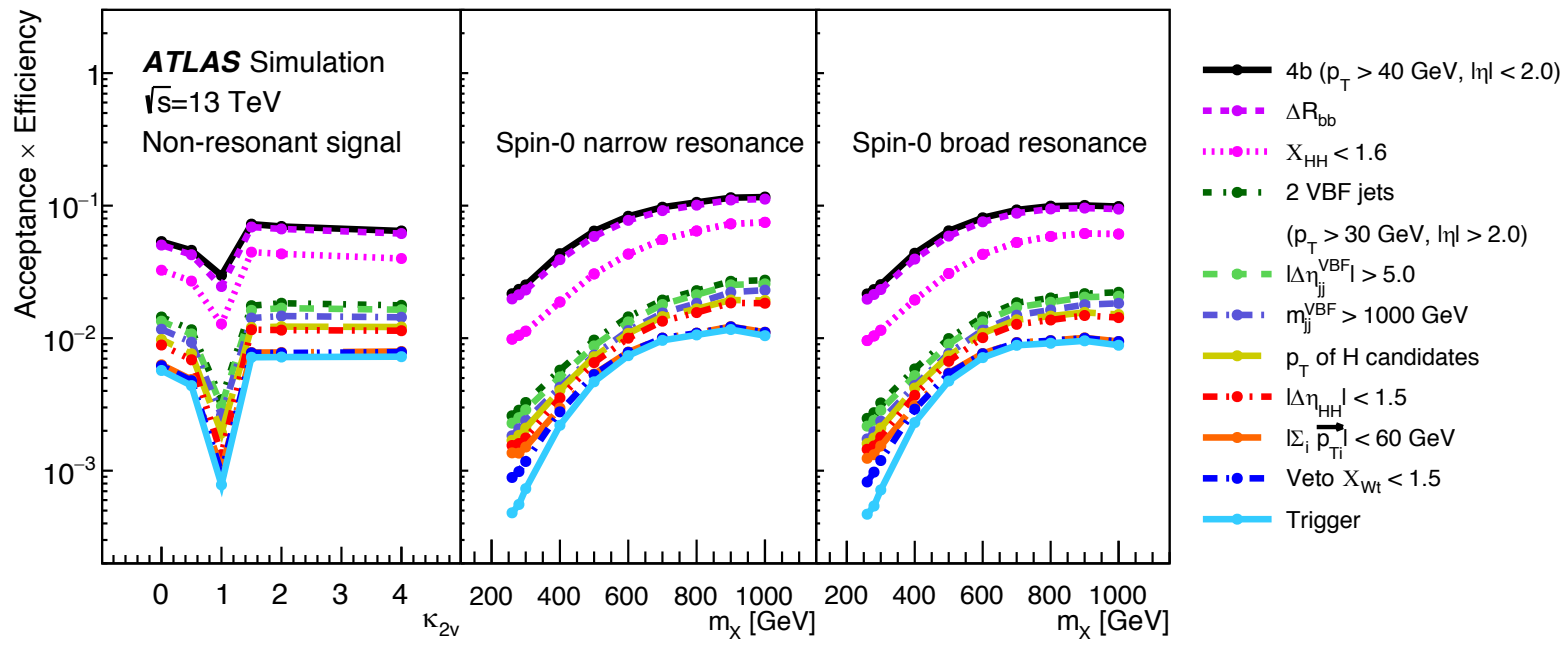
Detecting particles with ATLAS



VBF HH: acceptance x efficiency



arXiv:2001.05178

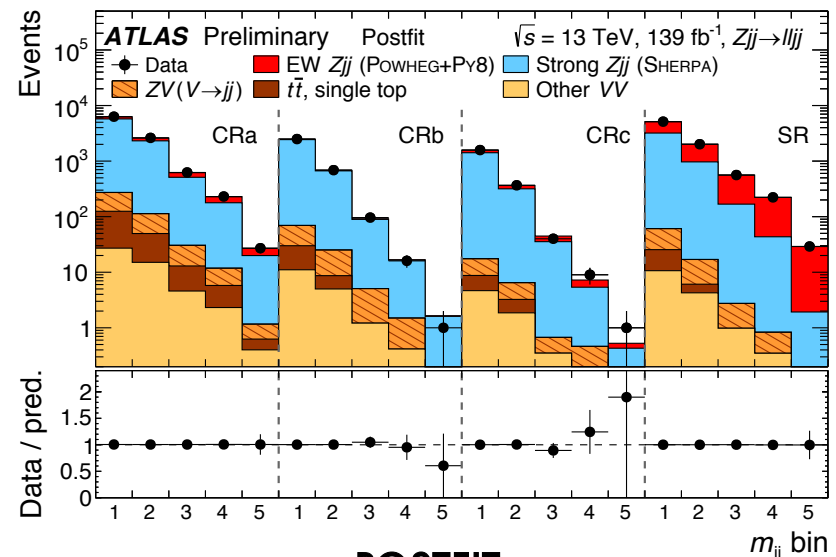
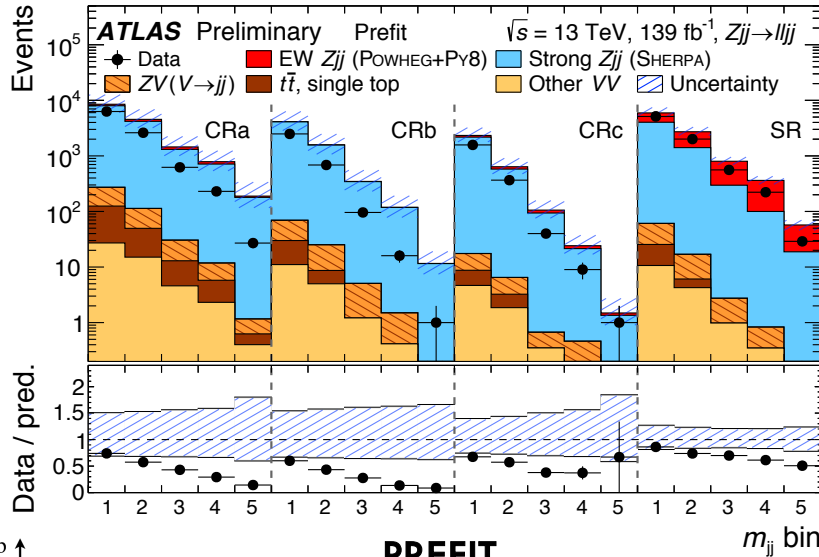
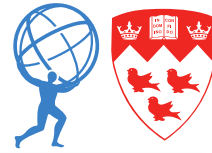


“For κ_{2V} values deviating from the SM prediction, growing non-cancellation effects result in a harder m_{HH} spectrum, and thereby higher- p_T b -jets, which in turn lead to increased signal acceptance times efficiency as shown in Figure 2.

This search is therefore not sensitive to the region close to the SM prediction, corresponding to $\kappa_{2V} = 1$ ”

Extracting the EW Z_{jj} signal

CERN-EP-2020-045



$N_{\text{jets}}^{\text{gap}}$	≥ 1	Strong Z_{jj} enhanced CRa	Strong Z_{jj} enhanced CRb
	$= 0$	EW Z_{jj} enhanced SR	Strong Z_{jj} enhanced CRc
		0.5	1.0

ξ_Z

PREFIT

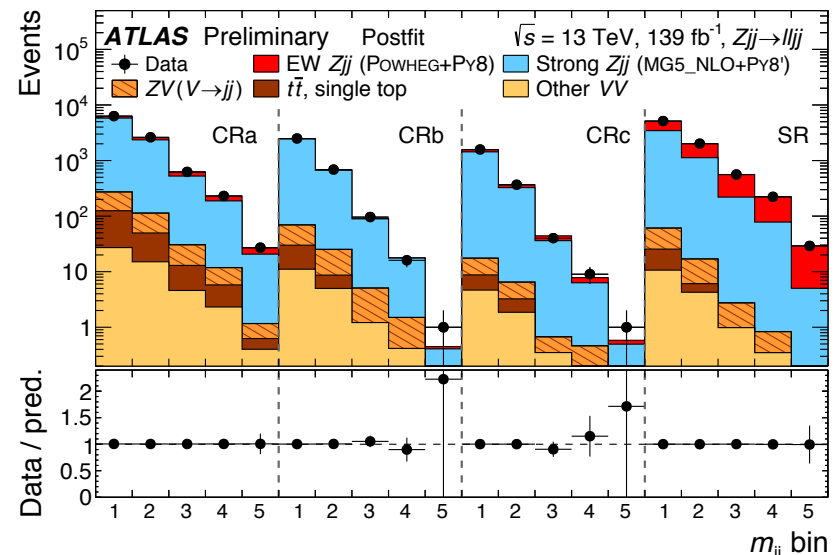
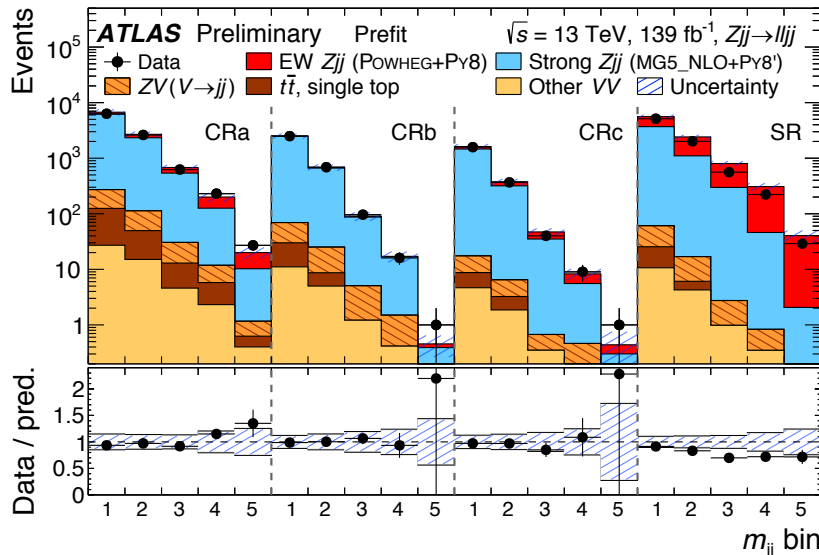
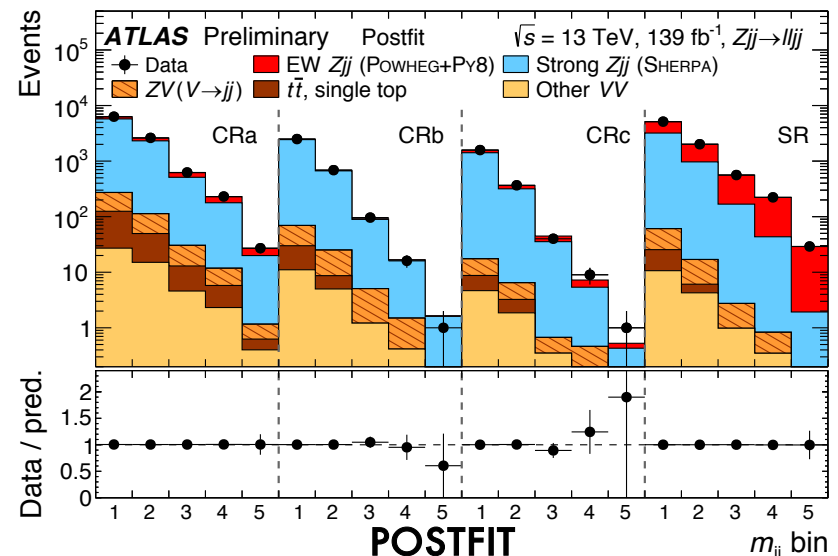
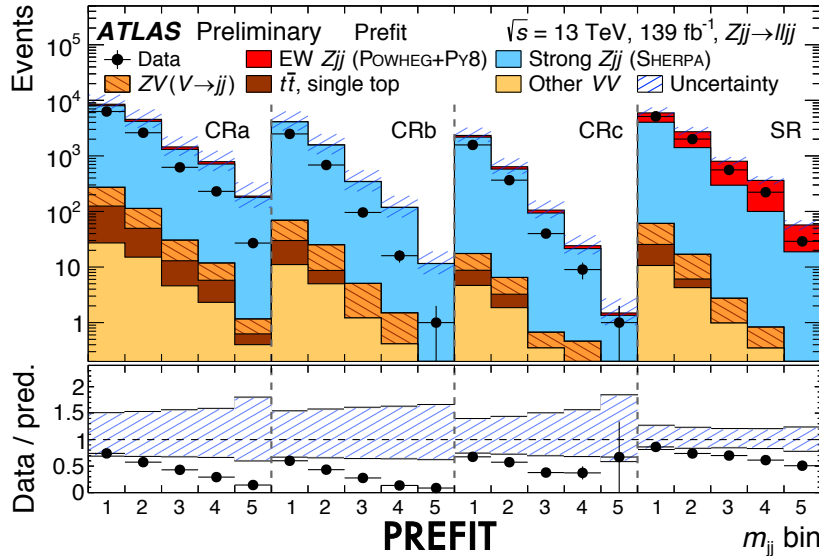
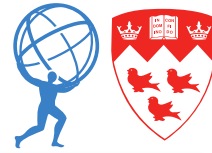
POSTFIT

Binned maximum likelihood fit is performed to reduce dependence on MC mismodelling, with $3 * N_{\text{bins}} + 2$ free parameters:

- (1) bin-by-bin weights for strong Z_{jj} , separate for low and high centrality but linked between $N_{\text{jets}}^{\text{gap}} \geq 1$ and $N_{\text{jets}}^{\text{gap}} = 0$
- (2) linear $f(x)$ applied to strong Z_{jj} to correct for residual $N_{\text{jets}}^{\text{gap}}$ dependence
- (3) bin-by-bin electroweak Z_{jj} signal strengths (same in all regions)

Extracting the EW Z_{ij} signal

CERN-EP-2020-045



➔ Perform fit again with alternative generators for strong Z_{ij} component